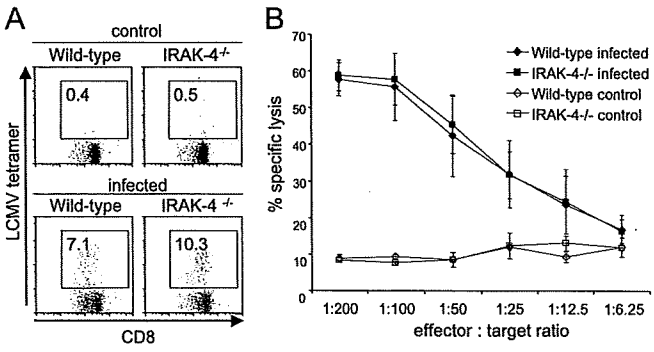

Figure 9. Responses of *IRAK-4*$^{-/-}$ T cells to LCMV infection. Wild-type and *IRAK-4*$^{-/-}$ mice were intravenously infected with 5×10^5 PFU of LCMV, and splenocytes were harvested at day 8 after infection. (A) The cells were stained with LCMV MHC class I tetramer and CD8a and were analyzed by flow cytometry. The data shown are representative of six different mice tested. (B) Ex vivo CTL activity in splenocytes was determined using 5-h ^{51}Cr release assay and GP33-loaded EL-4 cells as targets. Indicated values are mean ± SD of three mice. The data are representative of two separate experiments.

have not been well understood. Although it was shown that IRAK-4 phosphorylated IRAK-1 for activating TRAF6, TLR-mediated production of proinflammatory cytokines in *IRAK-1*$^{-/-}$ cells was not impaired in peritoneal macrophages. Further studies are required for identifying substrates other than IRAK-1 that are responsible for the TLR signaling pathway. Nevertheless, this is the first paper showing that the kinase activity of IRAK family members plays a critical role in their function in vivo.

The association between MyD88 and IRAK-4 was induced in response to IL-1β stimulation in both wild-type and *IRAK-4*$^{KN/KN}$ cells. A previous study showed that MyD88 interacted with kinase-negative, but not with wild-type, IRAK-4 when they were overexpressed in human embryonic kidney 293 cells (13). In contrast, it was reported that IL-1 stimulation induced an interaction between endogenous MyD88 and wild-type IRAK-4 (16). In that study, the kinase-truncated mutant of IRAK-4 was shown to constitutively interact with MyD88 even before IL-1 stimulation. Given that overexpression of wild-type IRAK-4 immediately activates NF-κB without further stimulation, the localization of overexpressed IRAK-4 may be different from endogenous protein. Based on our observation and that study (16), the endogenous IRAK-4 is probably recruited to MyD88 in response to stimulation, and IRAK-4 with KK213AA point mutation behaves similarly to wild-type IRAK-4 regarding association with MyD88.

Although IRAK-4 deficiency profoundly affected TLR2-mediated cytokine production, TNF-α gene induction was impaired, but not abrogated, as observed in MyD88 deficiency. TLR2-mediated expression of TNF-α and IκBζ genes was induced even in the absence of IRAK-4, though the expression in *IRAK-4*$^{-/-}$ and *IRAK-4*$^{KN/KN}$ cells was reduced and transient compared with wild-type cells. Furthermore, induction of NF-κB–DNA binding activity was also induced in *IRAK-4*$^{-/-}$ and *IRAK-4*$^{KN/KN}$ macrophages, although the activation was ~10 min delayed compared with wild-type cells. This finding is in contrast to the complete abrogation of TLR2 signaling in MyD88$^{-/-}$ macrophages and indicates the existence of an IRAK-4–independent signaling pathway. Stimulation with R-848 and CpG-DNA also induced NF-κB activation in an IRAK-4–independent manner without degrading IκBα, suggesting that the IRAK-4–independent pathway is not TLR2 specific. Given that the death domain of MyD88 is responsible for downstream signaling, other IRAK family members that contain an N-terminal death domain are candidates for mediating IRAK-4–independent signaling. Nevertheless, the activation of NF-κB in response to a TLR2 ligand was observed even in the absence of both IRAK-1 and -4. Because it was shown that IRAK-2 also positively regulated the IL-1β–signaling pathway, IRAK-2 may be responsible for the signaling pathway. Future studies will clarify if IRAK family members redundantly function in IL-1R/TLR responses in vivo. Although we clearly detected NF-κB–DNA binding activity, which is supershifted by anti-p50 and p65 Ab, we failed to detect activation of IKKs and phosphorylation of IκBα in the absence of IRAK-4 or its kinase activity in response to TLR2 stimulation. Induction of NF-κB activation without degradation of IκBα is quite unique, although the mechanism of activation is enigmatic. It has been reported that TLR2 stimulation leads to the recruitment of active Rac1 and phosphatidylinositol-3 kinase to the TLR2 cytosolic domain (27). Therefore, it is possible that the signaling is mediated through the small G protein–phosphatidylinositol-3 kinase pathway.

The TLR/IL-1R and antigen-receptor signaling share signaling molecules for activating NF-κB. In addition to IKK complex, TRAF6 was also reported to be involved in TCR-mediated NF-κB activation (28). TRAF6 can associate with MALT1, which forms a complex with BCL10 and CARMA1/CARD11. TRAF6 is oligomerized by the complex and activates IKKs by inducing polyubiquitination of IKK-γ/NF-κB essential modulator and activation of TGF-β–activated kinase 1. A recent paper showed that IRAK-4 was also involved in TCR responses via suppressing NF-κB activation by associating with ZAP-70 (18). However, the newly generated *IRAK-4*$^{-/-}$ mice did not show any defects in the T cell response as well as the TCR signaling pathway. Furthermore, IRAK-4 was not required for LCMV-induced CTL responses. *IRAK-4*$^{KN/KN}$ T cells also showed normal responses against TCR stimulation. We do not have a clear explanation for the discrepancy, and it may be due to the difference in the genetic background of the strains. However, it is unlikely that the critical TCR signaling components are different between mouse strains, suggesting that IRAK-4 is not critically involved in TCR signaling.

In summary, this study demonstrates that IRAK-4 activity plays a critical role in the physiological function of IRAK-4. Macrophages and DCs from *IRAK-4*$^{KN/KN}$ mice as well as *IRAK-4*$^{-/-}$ mice were profoundly defective in TLR-mediated

proinflammatory cytokine production. In addition, *IRAK-4*$^{KN/KN}$ mice were highly resistant to LPS-induced shock response. The exploration of small compounds targeting kinase activity of IRAKs has been challenged by the fact that expression of even kinase-inactive IRAK-4 mutant results in the activation of the intracellular signaling pathway. However, this study clearly indicates that the kinase activity of IRAK-4 is essential for the physiological functions, and the kinase activity of IRAK-4 is a good therapeutic target for inflammatory diseases and septic shock, without affecting acquired immune responses.

MATERIALS AND METHODS

Generation of *IRAK-4*$^{KN/KN}$ mice. The *IRAK-4* gene was isolated from genomic DNA extracted from ES cells (GSI) by PCR. A genomic fragment containing exon 2 of IRAK-4 was cloned into a pT7blue vector (Nugen), and point mutations resulting in the KK213AA conversion in the kinase domain were introduced by a site-directed mutagenesis. A targeting vector has a neomycin-resistance gene cassette (neo) flanked with two loxP sites, and a HSV thymidine kinase driven by PGK promoter was inserted into the genomic fragment for negative selection. The targeting vector was linearized and electroporated into ES cells (GSI). G418 and gancyclovir doubly resistant clones were selected and screened by PCR and further confirmed by Southern blotting. Three clones with homologous recombination were injected into blastocysts from C57BL/6 females, the obtained chimeric males were crossed with C57BL/6 females, and the obtained F1 generations with mutated IRAK-4 mice were crossed with CAG-Cre transgenic mice to excise the neo cassette. CAG-Cre transgene was removed from *IRAK-4*$^{KN/+}$ mice without a neo cassette by crossing the mice with C57BL/6 mice. *IRAK-4*$^{KN/+}$ mice were further intercrossed to obtain *IRAK-4*$^{KN/KN}$ mice. The *IRAK-4*$^{KN/KN}$ mice used were under 129Sv × C57BL/6 background. Mice were maintained in our animal facility and treated in accordance with the guidelines of Osaka University.

Generation of *IRAK-4*$^{-/-}$ mice. The *IRAK-4* gene was isolated from genomic DNA extracted from ES cells (GSI) by PCR. The targeting vector was constructed by replacing a 4.3-kb fragment encoding the *IRAK-4* ORF with a neo cassette, and a HSV thymidine kinase driven by PGK promoter was inserted into the genomic fragment for negative selection. After the targeting vector was transfected into ES cells, G418 and gancyclovir doubly resistant colonies were selected and screened by PCR and further confirmed by Southern blotting. Homologous recombinants were microinjected into blastocysts from C57BL/6 female mice, and heterozygous F1 progenies were intercrossed to obtain *IRAK-4*$^{-/-}$ mice. The *IRAK-4*$^{-/-}$ mice used were under 129Sv × C57BL/6 background.

Cells. Peritoneal exudate cells were isolated from the peritoneal cavity of mice 3 d after injection with 2 ml of 4.0% thioglycollate medium (Sigma-Aldrich) by washing with ice cold Hanks' balanced salt solution (Invitrogen). Bone-marrow DCs were prepared by cultivating either in the presence of 100 ng/ml human Flt3 ligand (PeproTech) or 10 ng/ml mouse GM-CSF (PeproTech) as described previously (29). Splenic T cells were isolated using MACS (Miltenyi Biotec).

Reagents. MALP-2 and PAM_3CSK_4 were synthesized as described previously (25, 26). LPS from *Salmonella minesota* Re-595 was purchased from Sigma-Aldrich. Poly I:C was purchased from GE Healthcare. R-848 was provided by the Pharmaceuticals and Biotechnology Laboratory of the Japan Energy Corporation. CpG oligonucleotide was synthesized as described previously (30). Polyclonal Ab to phosphorylated JNK (anti– phospho-JNK), anti–phospho-p38, anti–phospho-ERK, anti–phospho- IκBα (Ser32), and anti–phospho-NF-κB p65 (Ser536) were purchased from Cell Signaling. Polyclonal anti-JNK, anti-p38, anti-ERK, and anti–IκB-α were obtained from Santa Cruz Biotechnology, Inc. Abs to NF-κB p50 and p65 were purchased from Santa Cruz Biotechnology, Inc. Anti-MyD88 Ab was purchased from ProSci, and anti–IRAK-1 Ab was made as described previously (25). Rabbit anti–IRAK-4 polyclonal Ab was raised against a peptide corresponding to aa 436 to 459 of mouse IRAK-4. Specificity of this Ab was tested on overexpressed IRAK-4 (unpublished data) and on *IRAK-4*$^{-/-}$ cells (Fig. 1 D).

Measurement of cytokine production. Concentrations of cytokines in the culture supernatants were measured by ELISA. ELISA kits for mouse TNF-α, IL-6, IL-12 p40, and IL-2 were purchased from R&D Systems, and the kit for mouse IFN-α was purchased from PBL Biomedical Laboratories.

[^{3}H]thymidine uptake. Splenocytes were cultured with the indicated concentrations of MALP-2, poly I:C, LPS, CpG-DNA, anti-IgM (Jackson ImmunoResearch Laboratories), or anti-CD40 (BD Biosciences) for 48 h. For examining T cell responses, splenic T cells were activated with 10 μg/ml of plate-bound anti-CD3 (BD Biosciences) and 2 μg/ml of plate-bound anti-CD28 (BD Biosciences) for 48 h. Cells were pulsed with 1 μCi [^{3}H]thymidine for the last 16 h. [^{3}H]thymidine incorporation was measured by a scintillation counter (Packard Instrument Co.).

Synthesis of IRAK proteins and in vitro kinase assay. IRAK-4 cDNA was obtained by RT-PCR from mRNAs prepared from wild-type and *IRAK-4*$^{KN/KN}$ macrophages. The cDNAs were cloned into a pcDNA3 vector, which contains a T7 promoter and a Myc tag sequence. Recombinant Myc-tagged IRAK-4 proteins were expressed in the rabbit reticulocyte lysates using TNT T7 Quick coupled transcription/translation systems (Promega). A part of mouse IRAK-1 protein (aa 301–500), which contains the IRAK-1 activation loop, was also prepared the by same system. 10 μl of reticulocyte lysates, which contained recombinant kinase or exogenous substrate, was diluted with cell lysis buffer and combined as indicated. Kinase and substrate were immunoprecipitated with anti-Myc Ab (Cell Signaling), and then in vitro kinase assay was performed as described previously (31). For assessing autophosphorylation of endogenous IRAK proteins, peritoneal macrophages stimulated with 10 ng/ml MALP-2 were lysed and immunoprecipitated with anti–IRAK-1 and anti–IRAK-4 Ab. The kinase activity was then measured by in vitro kinase assay.

Northern blot analysis. Peritoneal macrophages were treated with 10 ng/ml MALP-2 for 0, 1, 2, 4, and 8 h, and total RNA was extracted using TRIzol reagent (Invitrogen). RNA was electrophoresed, transferred to nylon membranes, and hybridized with the indicated cDNA probes. To detect the expression of IRAK4 mRNA, a 394-bp fragment (707–1,101) was used as a probe. The same membrane was rehybridized with a β-actin probe.

Western blot analysis. Peritoneal macrophages were treated with 10 ng/ml MALP-2 for the indicated times. Cells were then lysed in a lysis buffer containing 1.0% NP-40, 150 mM NaCl, 20 mM Tris-Cl, pH 7.5, 1 mM EDTA, and protease inhibitor cocktail (Roche). Cell lysates were dissolved by SDS-PAGE and transferred onto a polyvinylidene difluoride membrane. The membrane was blotted with the specific Ab to indicated proteins and visualized with an enhanced chemiluminescence system (NEN Life Science Products). For immunoprecipitation, 10^7 MEFs were treated with 10 ng/ml IL-1β for the indicated periods, and cell lysates were immunoprecipitated with anti-MyD88 or anti–IRAK-4 Ab, followed by immunoblot with the indicated Abs.

EMSA. The nuclear extracts were prepared from peritoneal macrophages (5×10^6) stimulated with MALP-2 as described previously (4). Nuclear extracts were incubated with or without Abs against NF-κB p65 or p50, and then further incubated with a specific probe for NF-κB DNA binding sites, electrophoresed, and visualized by autoradiography.

Allogenic T cell response assay. The allogenic T cell responses were analyzed as described previously (32). In brief, bone marrow–derived DCs stimulated with 10 ng/ml MALP-2, 1 μg/ml LPS, or 100 nM CpG-DNA

for 48 h from BALB/c mice were harvested at day 8, irradiated at a dose of 30 Gy, and plated at threefold serial dilutions in 96-well round-bottom plates. These DCs were incubated for 3 d with 5×10^4/well of splenic $CD4^+$ T cells from wild-type, *IRAK4*$^{-/-}$, and *IRAK-4*$^{KN/KN}$ mice isolated using MACS with CD4 microbeads (Miltenyi Biotec). [^{3}H]thymidine was added for the last 16 h. [^{3}H]thymidine incorporation was measured by a scintillation counter.

LCMV infection and analysis of T cell responses. LCMV-WE strain was obtained from T. Otheki (Akita University, Akita, Japan). Wild-type and *IRAK4*$^{-/-}$ mice were intravenously infected with 5×10^5 PFU of LCMV-WE and splenocytes were harvested at day 8 after infection. To investigate the induction of LCMV-specific T lymphocytes, splenocytes were incubated with T-select H-2Db LCMV tetramer-KAVYNFATC-PE (MBL International Corporation) and CD8a-APC Ab. Samples were acquired on a FACS Calibur (BD Biosciences) and analyzed with FlowJo software (TreeStar).

For assessment of cytotoxicity of LCMV-specific T cells, splenocytes prepared from LCMV-infected mice were incubated for 5 h with EL-4 target cells that had been loaded with a peptide (GP33; KAVYNFATM; Peptide Institute) and labeled with ^{51}Cr. The percentage of specific lysis was calculated as [(experimental release − spontaneous release)/(maximal release − spontaneous release)] × 100%.

TNF bioassay. TNF activity was measured in macrophage culture supernatant after stimulation with MALP-2 for 1 and 2 h by cytotoxicity on L929 fibroblasts. L929 cells were plated on 96-well plates in RPMI 1640 medium supplemented with 2% FCS. Serial twofold dilutions of supernatants in 8 mg/ml actinomycin D were added to each well and incubated for 20 h. Viability of cells was determined using CellTiter-Glo (Promega) according to the manufacturer's instructions. Mouse recombinant TNF-α (R&D systems) was used to derive a standard curve, and the concentration of TNF-α was determined based on the standard curve.

Online supplemental material. Fig. S1 shows the generation of *IRAK-4*$^{-/-}$ mice. Fig. S2 shows the induction of TNF activity in response to MALP-2 stimulation. Fig. S3 shows that activation of NF-κB in response to MALP-2 was dependent on MyD88. Fig. S4 shows the activation of NF-κB in *IRAK-4*$^{-/-}$ and *IRAK-4*$^{KN/KN}$ macrophages in response to LPS, R-848, and CpG-DNA. Fig. S5 shows the proliferative responses of *IRAK-4*$^{-/-}$ and *IRAK-4*$^{KN/KN}$ T cells to soluble anti-CD3 plus anti-Ig Ab. Online supplemental material is available at http://www.jem.org/cgi/content/full/jem.20061523/DC1.

We thank all colleagues in our laboratory, M. Hashimoto for secretarial assistance, and Y. Fujiwara, M. Shiokawa, A. Shibano, and N. Kitagaki for technical assistance.

This work was in part supported by grants from the Ministry of Education, Culture, Sports, Science and Technology of Japan, from the 21st Century Center of Excellence Program of Japan, and from the National Institutes of Health (grant AI070167).

The authors have no conflicting financial interests.

Submitted: 19 July 2006
Accepted: 13 April 2007

REFERENCES

1. Akira, S., S. Uematsu, and O. Takeuchi. 2006. Pathogen recognition and innate immunity. *Cell.* 124:783–801.
2. Beutler, B. 2004. Inferences, questions and possibilities in Toll-like receptor signalling. *Nature.* 430:257–263.
3. Janeway, C.A., Jr., and R. Medzhitov. 2002. Innate immune recognition. *Annu. Rev. Immunol.* 20:197–216.
4. Yamamoto, M., S. Sato, H. Hemmi, K. Hoshino, T. Kaisho, H. Sanjo, O. Takeuchi, M. Sugiyama, M. Okabe, K. Takeda, and S. Akira. 2003. Role of adaptor TRIF in the MyD88-independent toll-like receptor signaling pathway. *Science.* 301:640–643.
5. Janssens, S., and R. Beyaert. 2003. Functional diversity and regulation of different interleukin-1 receptor-associated kinase (IRAK) family members. *Mol. Cell.* 11:293–302.
6. Croston, G.E., Z. Cao, and D.V. Goeddel. 1995. NF-kappa B activation by interleukin-1 (IL-1) requires an IL-1 receptor-associated protein kinase activity. *J. Biol. Chem.* 270:16514–16517.
7. Wesche, H., W.J. Henzel, W. Shillinglaw, S. Li, and Z. Cao. 1997. MyD88: an adapter that recruits IRAK to the IL-1 receptor complex. *Immunity.* 7:837–847.
8. Uematsu, S., S. Sato, M. Yamamoto, T. Hirotani, H. Kato, F. Takeshita, M. Matsuda, C. Coban, K.J. Ishii, T. Kawai, et al. 2005. Interleukin-1 receptor-associated kinase-1 plays an essential role for Toll-like receptor (TLR)7- and TLR9-mediated interferon-α induction. *J. Exp. Med.* 201:915–923.
9. Kanakaraj, P., P.H. Schafer, D.E. Cavender, Y. Wu, K. Ngo, P.F. Grealish, S.A. Wadsworth, P.A. Peterson, J.J. Siekierka, C.A. Harris, and W.P. Fung-Leung. 1998. Interleukin (IL)-1 receptor-associated kinase (IRAK) requirement for optimal induction of multiple IL-1 signaling pathways and IL-6 production. *J. Exp. Med.* 187:2073–2079.
10. Thomas, J.A., J.L. Allen, M. Tsen, T. Dubnicoff, J. Danao, X.C. Liao, Z. Cao, and S.A. Wasserman. 1999. Impaired cytokine signaling in mice lacking the IL-1 receptor-associated kinase. *J. Immunol.* 163:978–984.
11. Fitzgerald, K.A., E.M. Palsson-McDermott, A.G. Bowie, C.A. Jefferies, A.S. Mansell, G. Brady, E. Brint, A. Dunne, P. Gray, M.T. Harte, et al. 2001. Mal (MyD88-adapter-like) is required for Toll-like receptor-4 signal transduction. *Nature.* 413:78–83.
12. Kobayashi, K., L.D. Hernandez, J.E. Galan, C.A. Janeway Jr., R. Medzhitov, and R.A. Flavell. 2002. IRAK-M is a negative regulator of Toll-like receptor signaling. *Cell.* 110:191–202.
13. Li, S., A. Strelow, E.J. Fontana, and H. Wesche. 2002. IRAK-4: a novel member of the IRAK family with the properties of an IRAK-kinase. *Proc. Natl. Acad. Sci. USA.* 99:5567–5572.
14. Suzuki, N., S. Suzuki, G.S. Duncan, D.G. Millar, T. Wada, C. Mirtsos, H. Takada, A. Wakeham, A. Itie, S. Li, et al. 2002. Severe impairment of interleukin-1 and Toll-like receptor signalling in mice lacking IRAK-4. *Nature.* 416:750–756.
15. Suzuki, N., S. Suzuki, U. Eriksson, H. Hara, C. Mirtosis, N.J. Chen, T. Wada, D. Bouchard, I. Hwang, K. Takeda, et al. 2003. IL-1R-associated kinase 4 is required for lipopolysaccharide-induced activation of APC. *J. Immunol.* 171:6065–6071.
16. Medvedev, A.E., K. Thomas, A. Awomoyi, D.B. Kuhns, J.I. Gallin, X. Li, and S.N.Vogel. 2005. Cutting edge: expression of IL-1 receptor-associated kinase-4 (IRAK-4) proteins with mutations identified in a patient with recurrent bacterial infections alters normal IRAK-4 interaction with components of the IL-1 receptor complex. *J. Immunol.* 174:6587–6591.
17. Yang, K., A. Puel, S. Zhang, C. Eidenschenk, C.L. Ku, A. Casrouge, C. Picard, H. von Bernuth, B. Senechal, S. Plancoulaine, et al. 2005. Human TLR-7-, -8-, and -9-mediated induction of IFN-alpha/beta and -lambda is IRAK-4 dependent and redundant for protective immunity to viruses. *Immunity.* 23:465–478.
18. Suzuki, N., S. Suzuki, D.G. Millar, M. Unno, H. Hara, T. Calzascia, S. Yamasaki, T. Yokosuka, N.J. Chen, A.R. Elford, et al. 2006. A critical role for the innate immune signaling molecule IRAK-4 in T cell activation. *Science.* 311:1927–1932.
19. Knop, J., and M.U. Martin. 1999. Effects of IL-1 receptor-associated kinase (IRAK) expression on IL-1 signaling are independent of its kinase activity. *FEBS Lett.* 448:81–85.
20. Maschera, B., K. Ray, K. Burns, and F. Volpe. 1999. Overexpression of an enzymically inactive interleukin-1-receptor-associated kinase activates nuclear factor-kappaB. *Biochem. J.* 339:227–231.
21. Wesche, H., X. Gao, X. Li, C.J. Kirschning, G.R. Stark, and Z. Cao. 1999. IRAK-M is a novel member of the Pelle/interleukin-1 receptor-associated kinase (IRAK) family. *J. Biol. Chem.* 274:19403–19410.
22. Qin, J., Z. Jiang, Y. Qian, J.L. Casanova, and X. Li. 2004. IRAK4 kinase activity is redundant for interleukin-1 (IL-1) receptor-associated kinase phosphorylation and IL-1 responsiveness. *J. Biol. Chem.* 279:26748–26753.
23. Lye, E., C. Mirtsos, N. Suzuki, S. Suzuki, and W.C. Yeh. 2004. The role of interleukin 1 receptor-associated kinase-4 (IRAK-4) kinase activity in IRAK-4–mediated signaling. *J. Biol. Chem.* 279:40653–40658.
24. Honda, K., H. Yanai, T. Mizutani, H. Negishi, N. Shimada, N. Suzuki, Y. Ohba, A. Takaoka, W.C. Yeh, and T. Taniguchi. 2004. Role of a transductional-transcriptional processor complex involving MyD88

and IRF-7 in Toll-like receptor signaling. *Proc. Natl. Acad. Sci. USA.* 101:15416–15421.
25. Sato, S., O. Takeuchi, T. Fujita, H. Tomizawa, K. Takeda, and S. Akira. 2002. A variety of microbial components induce tolerance to lipopolysaccharide by differentially affecting MyD88-dependent and -independent pathways. *Int. Immunol.* 14:783–791.
26. Takeuchi, O., A. Kaufmann, K. Grote, T. Kawai, K. Hoshino, M. Morr, P.F. Muhlradt, and S. Akira. 2000. Cutting edge: preferentially the R-stereoisomer of the mycoplasmal lipopeptide macrophage-activating lipopeptide-2 activates immune cells through a toll-like receptor 2- and MyD88-dependent signaling pathway. *J. Immunol.* 164:554–557.
27. Arbibe, L., J.P. Mira, N. Teusch, L. Kline, M. Guha, N. Mackman, P.J. Godowski, R.J. Ulevitch, and U.G. Knaus. 2000. Toll-like receptor 2-mediated NF-kappa B activation requires a Rac1-dependent pathway. *Nat. Immunol.* 1:533–540.
28. Sun, L., L. Deng, C.K. Ea, Z.P. Xia, and Z.J. Chen. 2004. The TRAF6 ubiquitin ligase and TAK1 kinase mediate IKK activation by BCL10 and MALT1 in T lymphocytes. *Mol. Cell.* 14:289–301.
29. Hemmi, H., T. Kaisho, K. Takeda, and S. Akira. 2003. The roles of Toll-like receptor 9, MyD88, and DNA-dependent protein kinase catalytic subunit in the effects of two distinct CpG DNAs on dendritic cell subsets. *J. Immunol.* 170:3059–3064.
30. Hemmi, H., O. Takeuchi, T. Kawai, T. Kaisho, S. Sato, H. Sanjo, M. Matsumoto, K. Hoshino, H. Wagner, K. Takeda, and S. Akira. 2000. A Toll-like receptor recognizes bacterial DNA. *Nature.* 408:740–745.
31. Kawai, T., O. Adachi, T. Ogawa, K. Takeda, and S. Akira. 1999. Unresponsiveness of MyD88-deficient mice to endotoxin. *Immunity.* 11:115–122.
32. Kaisho, T., O. Takeuchi, T. Kawai, K. Hoshino, and S. Akira. 2001. Endotoxin-induced maturation of MyD88-deficient dendritic cells. *J. Immunol.* 166:5688–5694.

Regulation of innate antiviral defenses through a shared repressor domain in RIG-I and LGP2

Takeshi Saito*, Reiko Hirai†, Yueh-Ming Loo*, David Owen*, Cynthia L. Johnson*, Sangita C. Sinha‡, Shizuo Akira§, Takashi Fujita†, and Michael Gale, Jr.*¶

Departments of *Microbiology and ‡Internal Medicine, Division of Infectious Diseases, University of Texas Southwestern Medical Center, Dallas, TX 75235-9048; †Department of Genetics and Molecular Biology, Institute for Virus Research, Kyoto University, Kyoto 606-8507, Japan; and §Department of Host Defense, Research Institute for Microbial Diseases, Osaka University, Osaka 560-0043, Japan

Edited by Peter Palese, Mount Sinai School of Medicine, New York, NY, and approved November 1, 2006 (received for review August 3, 2006)

RIG-I is an RNA helicase containing caspase activation and recruitment domains (CARDs). RNA binding and signaling by RIG-I are implicated in pathogen recognition and triggering of IFN-α/β immune defenses that impact cell permissiveness for hepatitis C virus (HCV). Here we evaluated the processes that control RIG-I signaling. RNA binding studies and analysis of cells lacking RIG-I, or the related MDA5 protein, demonstrated that RIG-I, but not MDA5, efficiently binds to secondary structured HCV RNA to confer induction of IFN-β expression. We also found that LGP2, a helicase related to RIG-I and MDA5 but lacking CARDs and functioning as a negative regulator of host defense, binds HCV RNA. In resting cells, RIG-I is maintained as a monomer in an autoinhibited state, but during virus infection and RNA binding it undergoes a conformation shift that promotes self-association and CARD interactions with the IPS-1 adaptor protein to signal IFN regulatory factor 3- and NF-κB-responsive genes. This reaction is governed by an internal repressor domain (RD) that controls RIG-I multimerization and IPS-1 interaction. Deletion of the RIG-I RD resulted in constitutive signaling to the IFN-β promoter, whereas RD expression alone prevented signaling and increased cellular permissiveness to HCV. We identified an analogous RD within LGP2 that interacts in trans with RIG-I to ablate self-association and signaling. Thus, RIG-I is a cytoplasmic sensor of HCV and is governed by RD interactions that are shared with LGP2 as an on/off switch controlling innate defenses. Modulation of RIG-I/LGP2 interaction dynamics may have therapeutic implications for immune regulation.

hepatitis C virus | IFN | IPS-1 | MAVS | Cardif

Virus infection of mammalian cells triggers innate immune defenses through pathogen recognition receptors (PRRs) of the host that bind to pathogen-associated molecular patterns (PAMPs) within viral products and engage intracellular signaling pathways to initiate an antiviral response. Viral RNA is a potent inducer of this host response and is recognized by specific Toll-like receptors or by the cytoplasmic RNA helicases RIG-I and MDA5 (1). RIG-I and MDA5 are unique among the helicases because they contain tandem caspase activation and recruitment domains (CARDs) (2, 3). Both RIG-I and MDA5 bind to the synthetic double-stranded (ds)RNA poly inosine:cytosine (pIC), albeit with distinct efficiencies (4, 5). Studies of human cells defective in RIG-I signaling, or of cells from mice with a targeted deletion of Rig-I or Mda5, have revealed remarkable specificity of virus recognition between each helicase that could reflect their distinctions in RNA binding and PRR function. In particular, RIG-I is essential for triggering the host response to Sendai virus (SenV) and hepatitis C virus (HCV), whereas MDA5 has been shown to be important for the response to picornaviruses (5, 6). RIG-I and MDA5 initiate the host response by binding to IPS-1 (7). IPS-1, also known as Cardif, MAVS, and VISA (reviewed in ref. 8), is a CARD family protein that mediates CARD-dependent interactions with RIG-I and MDA5. These interactions stimulate IPS-1 signaling of downstream IFN regulator factor 3 (IRF-3) and NF-κB transcription factors that induce IFN-α/β production and IFN-stimulated genes that suppress virus infection (1). Control of virus signaling is mediated in part by LGP2, a related helicase that lacks CARDs but binds dsRNA (4, 9). However, the mechanisms of this regulation are not defined. Expression of RIG-I, MDA5, and LGP2 is induced by IFN, although RIG-I is basally expressed at a low level in most tissues. RIG-I is silent in the cell until it engages dsRNA, but the signaling activity of the RIG-I CARDs is unmasked upon deletion of the C-terminal helicase domain (2, 6). These observations suggest that RIG-I is initially autoregulated by its C terminus and then subjected to transregulation by LGP2 when IFN is produced during the latter stages of the host response.

Misregulation of RIG-I could be expected to deleteriously influence the antiviral host response. An example of this comes from HCV, to which the RIG-I-dependent host response limits virus replication and spread (6, 10). HCV is a single-stranded RNA virus whose genome is punctuated with dsRNA structures within the 5′ and 3′ nontranslated region (NTR) that alone can trigger RIG-I signaling and the host response in cultured cells (6). HCV overcomes this response through viral NS3/4A protease cleavage of IPS-1 to ablate RIG-I signaling of IRF-3 activation and the host response *in vivo*, thus providing a foundation for chronic infection in nearly 200 million people (11, 12). Processes that control RIG-I signaling may similarly impact adaptive immunity, because α/β IFNs are essential for sustaining T cell expansion and memory formation during virus infection (13). The present study was conducted to define PRR function and regulatory processes of RIG-I and MDA5 signaling and their points of control by LGP2. We identified a repressor domain (RD) of CARD signaling whose actions impact HCV infection and immunity.

Results

RIG-I and LGP2 Bind HCV RNA. To define the functional domains of RIG-I and their relationship with homologous regions of MDA5 and LGP2, we created a panel of wild-type (WT) and mutant expression constructs, including an extensive set of RIG-I mutants (Fig. 1*A*). We analyzed Flag-tagged construct binding to the synthetic dsRNA, pIC, and HCV RNA by using sensitive RNA-binding/agarose bead pull-down assays to recover RIG-I from

Author contributions: T.S., R.H., C.L.J., T.F., and M.G. designed research; T.S., R.H., Y.-M.L., D.O., C.L.J., S.C.S., T.F., and M.G. performed research; T.S., Y.-M.L., S.A., and M.G. contributed new reagents/analytic tools; T.S., D.O., C.L.J., S.C.S., T.F., and M.G. analyzed data; and T.S. and R.H. wrote the paper.

The authors declare no conflict of interest.

This article is a PNAS direct submission.

Abbreviations: CARD, caspase activation and recruitment domain; HCV, hepatitis C virus; IRF-3, IFN regulator factor 3; MEFs, mouse embryo fibroblasts; NTR, nontranslated region; PAMP, pathogen-associated molecular pattern; pIC, poly inosine:cytosine; PRR, pathogen recognition receptor; RD, repressor domain; SenV, Sendai virus.

¶To whom correspondence should be addressed at: Department of Microbiology, University of Texas Southwestern Medical Center, 5323 Harry Hines Boulevard, Dallas, TX 75235-9048. E-mail: michael.gale@utsouthwestern.edu.

This article contains supporting information online at www.pnas.org/cgi/content/full/0606699104/DC1.

www.pnas.org/cgi/doi/10.1073/pnas.0606699104

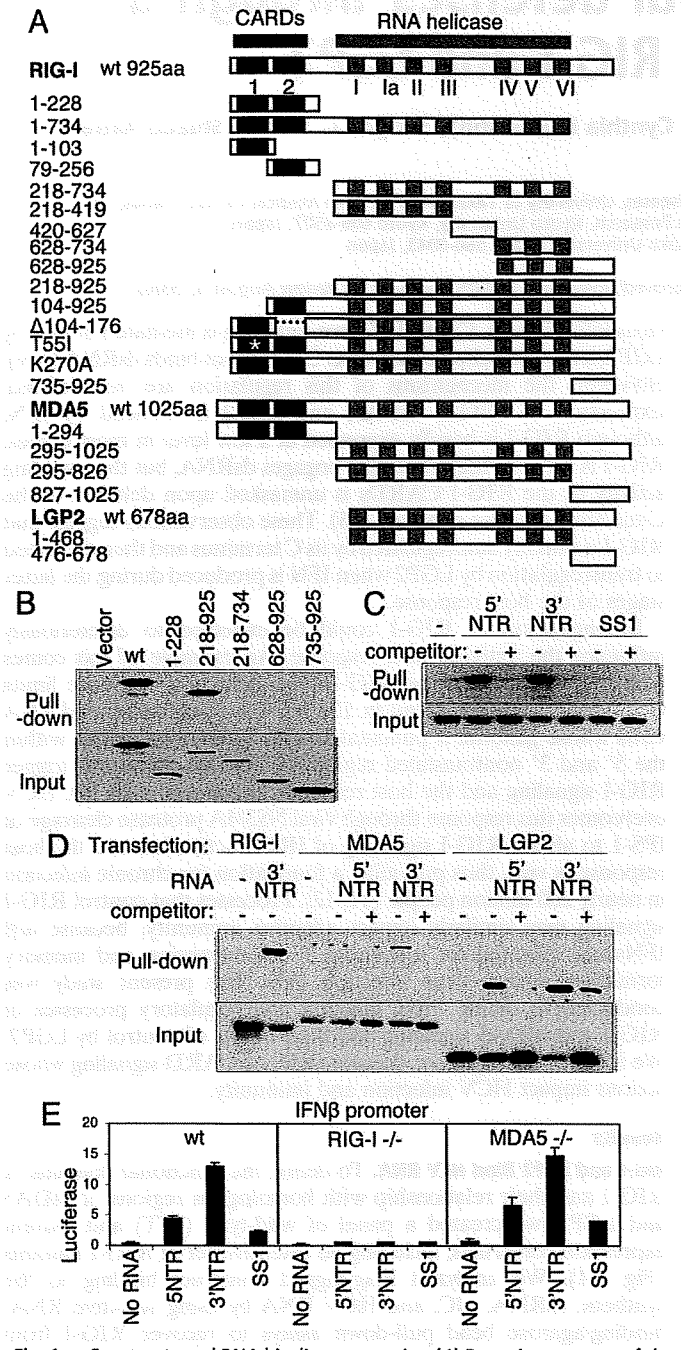

Fig. 1. Constructs and RNA binding properties. (*A*) Domain structure of the RIG-I, MDA5, and LGP2 constructs showing the positions of the tandem CARDs and the RNA helicase domain and its subdomains conserved among the helicase superfamily (15). Point mutations are indicated by an asterisk. The amino acid region encoded by each construct is shown at left. (*B*) Extract from Huh 7 cells that were transfected with empty vector or plasmid expressing Flag-tagged RIG-I constructs encoding WT (wt) RIG-I or the indicated amino acid regions of RIG-I were mixed with pIC-agarose beads and subjected to pull-down assay for dsRNA binding. RIG-I proteins within the input material (*Lower*) and recovered as pull-down product (*Upper*) were evaluated by immunoblotting using anti-Flag antibody. (*C* and *D*) Cytoplasmic fraction (20 μg) from 293 cells transfected with plasmid encoding Flag-tagged WT RIG-I (*C*) or with Flag RIG-I wt, Flag-MDA5 wt, or Flag-LGP2 wt (*D*) were mixed with 1 μg of *in vitro*-transcribed biotin-UTP HCV 5′ NTR RNA, 3′ NTR RNA, or SS1 RNA alone (−) or with an excess of unlabeled homologous competitor RNA (+). RNA–protein complexes were recovered by pull-down assay using streptavidin affinity gel. Flag-tagged protein within the pull-down fraction or 25% of input material was analyzed by immunoblotting using anti-Flag antibody. (*E*) wt, RIG-I-null, or MDA5-null MEFs were cotransfected with plasmids encoding constitutive *Renilla* luciferase and firefly luciferase controlled by the murine IFN-β promoter (2). After 24 h, the cells were mock-transfected or transfected with 10 ng of *in vitro*-transcribed, gel-purified RNA encoding the HCV 5′ NTR, 3′ NTR, or SS1 region (6). After 24 h, the cells were harvested, and extracts were subjected to dual luciferase assay. Bars show relative luciferase values and SD.

Huh7 cell extracts (6). WT RIG-I and its C-terminal region of amino acids 218–925 were recovered from cell extracts by using pIC-agarose beads (Fig. 1*B*). We also found that a Walker-A/ATPase-deficient mutant (RIG-I K270A) retained dsRNA binding function (data not shown). However, RIG-I constructs encoding helicase domain fragments or amino acids 735–925 alone failed to bind pIC, demonstrating that dsRNA binding requires both the RIG-I helicase domain and C terminus. RIG-I formed a specific complex with *in vitro*-transcribed HCV RNA encoding the highly structured 5′ or 3′ NTR but did not bind to the same length SS1 RNA (6), a defined linear, nonstructured domain of the HCV genome (14) (Fig. 1*C*). Similar analyses revealed efficient HCV NTR RNA binding by LGP2 and demonstrated that MDA5 binds only weakly to HCV 3′ NTR RNA (Fig. 1*D*). We confirmed that RIG-I and LGP2 could bind HCV genomic RNA [see supporting information (SI) Fig. 5*A*]. These results indicate that RIG-I binds to dsRNA or 2° structured RNA, including HCV RNA, through its helicase domain and C terminus independently of its CARDs, and binding efficiency is shared by LGP2 but not MDA5. We further evaluated the functional role of MDA5 and RIG-I in IFN-β promoter signaling by HCV RNA. When transfected into WT control mouse embryo fibroblasts (MEFs), HCV NTR RNA but not SS1 RNA triggered signaling processes that activated the IFN-β promoter. This response was absent in RIG-I-null MEFs but remained intact in MDA5-null MEFs (Fig. 1*E*). Similar results were obtained when MEFs were transfected with HCV genome RNA (SI Fig. 5*B*). These results define RIG-I as a dsRNA-binding protein and PRR for HCV RNA.

dsRNA and ATP Analog Promote Formation of a Trypsin-Resistant 30-kDa Domain of RIG-I. Conformational change induced by dsRNA could be a mechanism of RIG-I signaling activation. We therefore determined the trypsin sensitivity of recombinant RIG-I. Purified recombinant RIG-I produced in insect cells exhibited binding activity to 25-bp synthetic dsRNA ligand as determined by gel shift assay (SI Fig. 5*C*). The C-terminal portion of RIG-I, as detected by a mAb whose epitope mapped to amino acids 477–925, was highly sensitive to trypsin digestion in the absence of dsRNA ligand. However, the association of RIG-I with dsRNA and 5′-adenylyl-imidodiphosphate (AMP-PNP), a nonhydrolyzable ATP analog, conferred limited resistance to trypsin digestion and resulted in the generation of a trypsin-resistant 30-kDa polypeptide (Fig. 2*A*). Thus, upon binding dsRNA ligand, and in the presence of bound nucleotide, RIG-I may undergo a conformational change that displaces its C-terminal region. Because dsRNA triggers RIG-I signaling, C-terminal conformation changes induced by dsRNA could presumably confer RIG-I signaling activation during virus infection.

RIG-I Signaling and IPS-1 Interaction Require Tandem CARDs and Are Controlled by a C-Terminal RD. To determine the RIG-I requirements for host response signaling, we measured luciferase levels driven by the IFN-β promoter (Fig. 2*B*) or by the NF-κB-responsive PRDII promoter element (11, 12) during SenV infection of cells expressing RIG-I constructs (see SI Fig. 6). Ectopic WT RIG-I enhanced SenV-induced promoter activation, and RIG-I signaling required both intact CARDs in tandem (Fig. 2*B* and SI Fig. 6 *A* and *B*). Constructs encoding only the first or second CARD failed to signal IFN-β promoter induction (SI Fig. 6*B*) but lacked dominant-negative activity. The latter was a property of constructs lacking either CARD alone in the context of the full-length protein.

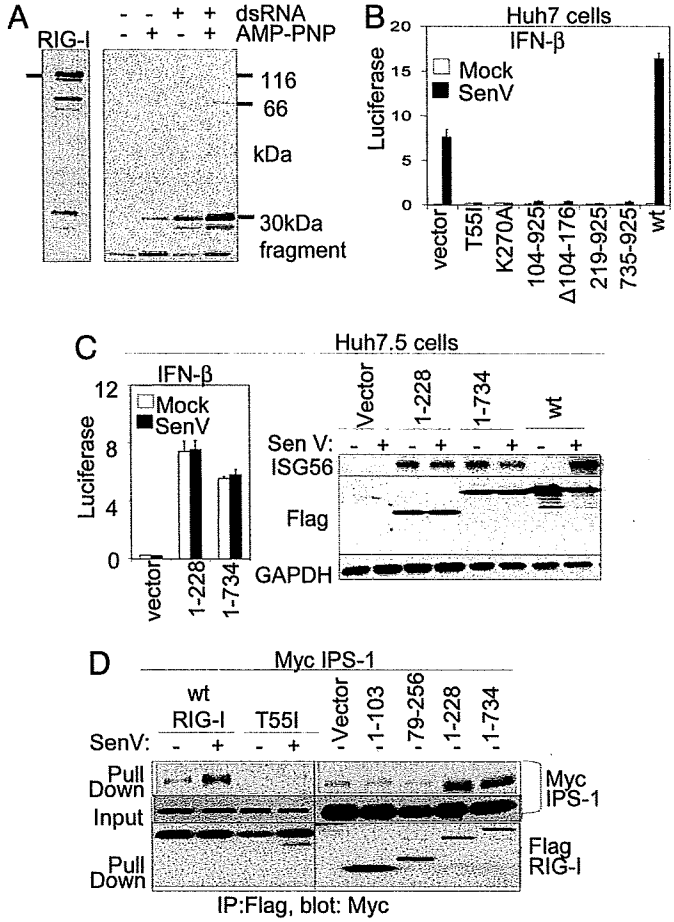

Fig. 2. An RD controls RIG-I signaling. (*A*) Recombinant RIG-I protein was digested with trypsin in the presence or absence of dsRNA and AMP-PNP as indicated. After termination of the reaction, the mixtures were analyzed by immunoblotting using anti-RIG-I mAb, which reacts with the C-terminal portion of RIG-I. Bars indicate the undigested 115-kDa RIG-I input protein (*Left*) and a 30-kDa protected digestion fragment (*Right*). (*B*) Huh 7 cells were cotransfected with luciferase promoter constructs and the indicated RIG-I expression constructs. After 24 h, the cells were mock-infected or infected with SenV. Cells were harvested 20 h later for dual luciferase assay. Bars show the mean relative IFN-β promoter–luciferase levels (± SD). (*C*) Huh 7.5 cells were cotransfected with promoter luciferase plasmids and empty vector or the indicated RIG-I expression plasmids. Cells were mock- or SenV-infected as indicated and were processed as above for dual luciferase assay (*Left*) or were harvested and analyzed by immunoblot assay for ISG56, Flag-RIG-I construct (Flag), and GAPDH abundance as shown (*Right*). (*D*) Huh7.5 cells were cotransfected with plasmids encoding Myc-IPS-1 and vector control or the indicated RIG-I constructs. After 16 h, the cells were mock-infected or infected with SenV as shown, cultured for 16 h, and harvested for anti-Flag immunoprecipitation (IP) and immunoblot assays as described in ref. 10. Shown are Flag-RIG-I protein abundance in the input material (*Bottom*) and Myc-IPS within the IP product (*Top*) or input material (*Middle*).

Moreover, the RIG-I T55I and K270A point mutations respectively disrupt CARD function and ATP binding/ATPase activity (2, 6), and they each exhibit dominant-negative control of RIG-I signaling (Fig. 2*B* and SI Fig. 6*A*). RIG-I amino acids 735–925 were also dominant-negative for signaling when expressed in Huh7 (Fig. 2*B*) or 293 cells (SI Fig. 6*A*). When expressed in Huh7.5 cells, which harbor a dominant-negative mutant RIG-I allele that prevents signaling by RIG-I (6), RIG-I 1–735 alone conferred constitutive promoter signaling and expression of endogenous ISG56, in a manner similar to ectopic expression of RIG-I 1–228 encoding the tandem CARDs alone (Fig. 2*C*). We conclude that RIG-I mutants devoid of signaling activity but that encode an intact C terminus exhibit dominant-negative function, whereas deletion of the C terminus (amino acids 735–925) renders RIG-I constitutively active.

We conducted coimmunoprecipitation analyses to define the control points and requirements for RIG-I/IPS-1 binding. Importantly, we found that complex formation was induced upon virus infection (Fig. 2*D*). Although WT RIG-I formed a virus-induced complex with IPS-1, the interaction depended on the tandem RIG-I CARDs and was disrupted by the RIG-I T55I mutation. RIG-I constructs encoding amino acids 1–228 or 1–734, respectively lacking the entire helicase domain and C terminus or lacking the C terminus only (see Fig. 1*A*), formed a constitutive complex with IPS-1 independently of virus infection, consistent with the signaling properties of each RIG-I mutant (compare Fig. 2 *C* and *D*). Thus, both RIG-I CARDs are required for downstream signaling and interactions with IPS-1 through a process that is negatively regulated by the RIG-I C terminus. Taken together, these results define RIG-I amino acids 735–925 as an RD that controls innate defense signaling, possibly by governing RIG-I interactions.

RIG-I Signals as a Multimeric Complex Regulated by RD Interactions. To determine the mechanisms of RD regulation of RIG-I signaling, we examined RIG-I complex formation and the influence of the RD in this process. Multimerization is a hallmark of CARD proteins (1). We therefore conducted coupled native PAGE/immunoblot analyses to determine whether RIG-I multimerizes as it signals downstream IRF-3 activation during virus infection. SenV infection of Huh7 cells induced endogenous RIG-I complex formation and concomitant dimerization of IRF-3 (Fig. 3*A*). RIG-I constitutively formed a complex when overexpressed but signaled IRF-3 activation and dimerization only after SenV infection. Ectopic expression of the RIG-I RD alone prevented complex formation of endogenous WT RIG-I and concomitantly blocked SenV-induced IRF-3 dimerization. Moreover, we found that when expressed alone, the RD was sufficient to prevent SenV-induced RIG-I interaction with IPS-1 in coimmunoprecipitation assays (Fig. 3*B*).

We further assessed complex formation between epitope-tagged WT and mutant RIG-I constructs. As shown in Fig. 3*C*, WT Flag-RIG-I was recovered as a complex with WT Myc-RIG-I that was stimulated by SenV infection, whereas Flag-RIG-I 1–228 formed a stable complex with WT Myc-RIG-I irrespective of virus infection. In further studies we found that RIG-I 1–228 does not self-associate (SI Fig. 6*C Left*) and that expression of RIG-I 1–228 induced the IFN-β promoter in WT MEFs but failed to induce promoter activity in RIG-I null MEFs (SI Fig. 6*C Right*), suggesting that RIG-I 1–228 constitutive signaling activity is mediated by heterocomplex with WT RIG-I independently of self CARD-CARD association. The dominant-negative Flag-RIG-I constructs encoding the helicase domain and C terminus (amino acids 218–925) or the RD alone (amino acids 735–925) each formed a constitutive complex with WT Myc-RIG-I (Fig. 3*C*), suggesting that these constructs prevent signaling by forming an RD trans inhibitory complex with WT RIG-I. In support of this, coimmunoprecipitation experiments demonstrated RD interactions with the RIG-I amino acids 1–228 encoding the tandem CARDs, and also demonstrated interaction with the helicase domain that mapped to within amino acids 420–627 corresponding to the linker region between helicase subdomains III and IV (15) (Figs. 3*D* and 1*A*). The expression of the RD was inhibitory for signaling by WT RIG-I but not by the tandem RIG-I CARDs alone (SI Fig. 6*D*). Taken together, these results indicate that (*i*) RIG-I signals as a self-complex whose actions are directed by tandem CARDS and induced by virus infection, and (*ii*) RIG-I signaling is negatively regulated through internal RD interactions that control self-association and interaction with IPS-1.

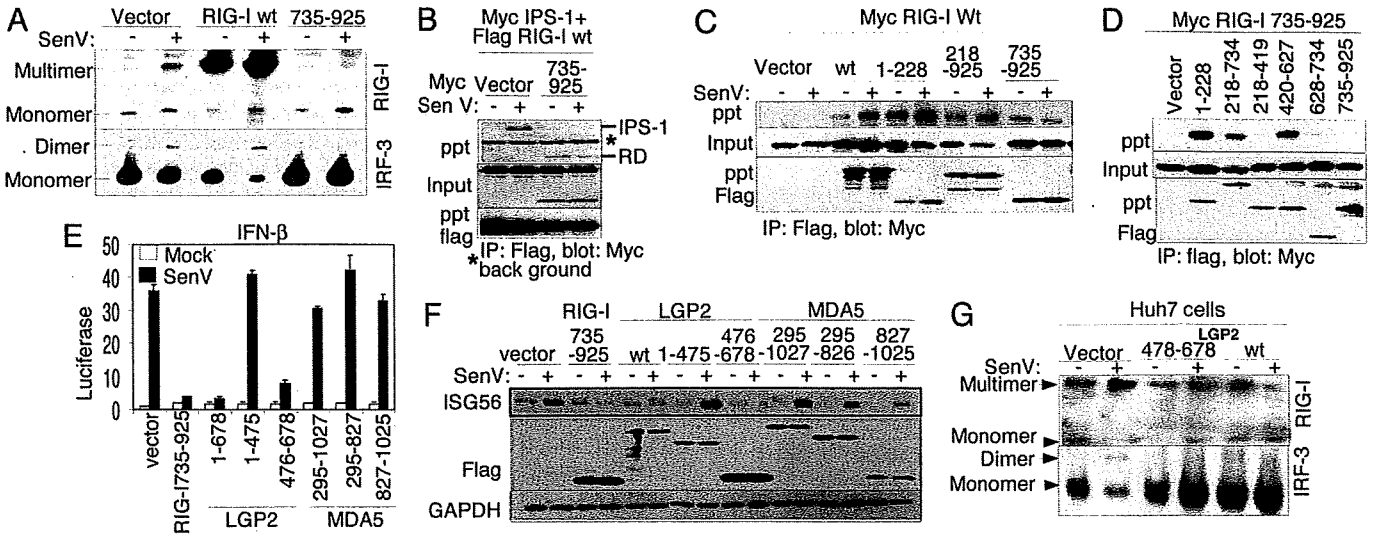

Fig. 3. Mechanism of regulation by the RIG-I RD. Where indicated, cells were mock-infected or infected with SenV for 16 h before harvesting. (*A*) Stable Huh7 cell lines expressing vector alone, RIG-I wt, or RIG-I 735–925 were mock-infected or infected with SenV, and protein extracts were subjected to native PAGE and immunoblot analysis with anti-RIG-I antibody (*Upper*) or anti-IRF-3 antibody (*Lower*). Dimer/multimer and monomer protein forms are indicated. (*B–D*) Huh7 cells were cotransfected with plasmids encoding Myc-IPS-1, Flag-RIG-I wt, and vector or Myc-RIG-I 735–925 (*B*); Myc-RIG-I wt and the indicated Flag construct (*C*); or Myc-RIG-I 735–925 and the indicated Flag construct (*D*). Cells were infected as shown and harvested, and extracts were analyzed by immunoprecipitation (IP) and immunoblot assays. Shown are the abundance of Myc-tagged protein within anti-Flag IP products (*Top*), input Myc-tagged protein (*Middle*), and input Flag-tagged protein (*Bottom*). (*E* and *F*) Huh 7 cells were transfected with *Renilla* luciferase, IFN-β-luciferase plasmids, and plasmids encoding vector alone or the indicated Flag-tagged RIG-I, LGP2, or MDA5 constructs. After SenV infection, the cells were harvested and extracts were subjected to dual luciferase assay (*E*) (bars show relative luciferase and SD) and to immunoblot assay for abundance of ISG56, Flag-tagged protein (Flag), and GAPDH (*F*). (*G*) Anti-RIG-I (*Upper*) or anti-IRF-3 (*Lower*) immunoblot of Huh7 cell extracts separated by native PAGE. Protein monomer and multimer/dimer forms are indicated. Cells were transfected with vector control or expression plasmid encoding Flag-LGP2 478–378 or Flag-LGP2 wt. Extracts were prepared after SenV or mock infection.

RD Function Is a Common Feature of RIG-I and LGP2 but Not MDA5. RIG-I shares a level of sequence similarity with MDA5 and LGP2 throughout their respective C-terminal regions and has been shown to block RIG-I signaling (4). We therefore assessed signaling regulation to the IFN-β promoter (Fig. 3*E*) and endogenous ISG56 expression (Fig. 3*F*) by WT or truncation mutants of RIG-I, LGP2, and MDA5. LGP2 prevented SenV induction of the IFN-β promoter and ISG56 expression in a manner similar to the RIG-I RD, and this was attributed to LGP2 C-terminal amino acids 476–678 independently of its helicase domain. In contrast, ectopic WT MDA5 expression constitutively induced IFN-β promoter activity irrespective of its C-terminal region or SenV infection (SI Fig. 6*E*). Truncation constructs of MDA5 lacking the CARDs (amino acids 322–1027) or encoding amino acids 827–1025, analogous to the RIG-I RD, were inert and neither stimulated nor blocked SenV induction of the IFN-β promoter or ISG56 expression (Fig. 3 *E* and *F*). Coimmunoprecipitation experiments demonstrated that WT LGP2 or LGP2 476–678 could form a stable complex with WT RIG-I or WT MDA5 when overexpressed in Huh7 cells (SI Fig. 6*F*). However, when coexpressed in Huh7. 5 cells neither WT LGP2 (see SI Fig. 7) nor the LGP2 RD (data not shown) could block constitutive signaling mediated by RIG-I 1–228 or MDA5. Together, these results suggest that (*i*) LGP2 controls signaling by RIG-I but not MDA5 through interactions between the RIG-I helicase domain and an RD encoded by amino acids 476–678 of LGP2, (*ii*) the analogous region of MDA5 does not harbor RD function, and (*iii*) the LGP2 interaction does not block signaling by MDA5. When expressed alone in Huh7 cells, the LGP2 RD functioned in a manner similar to WT LGP2 to block both SenV induction of endogenous RIG-I self-association and subsequent IRF-3 dimer formation (Fig. 3*G*)

RIG-I Signaling and Cell Permissiveness for HCV Are Governed by the RD. To determine the functional role of the RIG-I RD in regulating PRR signaling and host control of virus infection, we analyzed a set of Huh7 cell lines that constitutively express the RIG-I RD (Huh7-RIG-I-735–925) or WT RIG-I (Huh7-RIG-I-wt). We compared their host response and virus infection phenotype with Huh7 control cells and with Huh7.5 cells. The latter are highly permissive to HCV (6, 10, 16). SenV infection triggered the IFN-β promoter and ISG56 expression in Huh7 cells and Huh7-RIG-I-wt cells but stimulated neither IFN-β nor ISG56 expression in Huh7.5 cells or Huh7-RIG-I-735–925 cells (see SI Fig. 8). We also assessed the relative permissiveness of each cell line to HCV infection, with the JFH1 strain genotype 2a HCV infectious clone (17). HCV infection triggers the host response through a RIG-I-dependent process that limits initial permissiveness of Huh7 cells for infection (6, 10). Analysis of infected cultures demonstrated marked differences in infected cell numbers, viral protein abundance, and infectious virus production. Huh7 cells were less permissive for HCV infection than Huh7.5 cells. When compared with Huh7 control cells, expression of the RD in Huh7-RIG-I-735–925 cells conferred enhanced permissiveness for infection, increased viral protein abundance, and higher levels of infectious virus production (Fig. 4 *A–C*, respectively). In contrast, Huh7-RIG-I-wt cells exhibited reduced HCV permissiveness and virus production, consistent with RIG-I enhancement of host defenses. We note that Huh7.5 cells overall showed the highest permissiveness to HCV infection, implying that additional features act with the RIG-I deficiency to effect high permissiveness for HCV. We conclude that RD control of the RIG-I pathway and host defense signaling is an important determinant of cellular permissiveness to HCV infection.

Discussion

In this study, structure–function analyses of RIG-I revealed dsRNA PAMP binding and an induced conformation shift that associates with RIG-I PRR signaling actions. We found that RIG-I signaling requires the full tandem CARD arrangement, that it likely signals as a multimeric complex, and that an RD in RIG-I and LGP2 tightly regulates CARD signaling actions. Native gel analyses showed that,

although RIG-I resides as a monomer in resting cells, virus infection or high levels of expression promote its self-association. Thus, RIG-I signals through its tandem CARDs as a multimeric complex. Further support for this idea comes from two sets of observations. First, deletion of either CARD alone ablated RIG-I signaling actions. Second, the RIG-I T55I mutant formed a complex with WT RIG-I that ablated IPS-1 binding and downstream signaling (see Fig. 2 and SI Fig. 6). RIG-I constructs lacking either CARD were also dominant-negative for signaling. Together, this indicates that RIG-I signals at least as a dimeric unit in which residue T55, located within the first CARD, might participate in IPS-1 interaction. In addition, we found that MDA5 also forms a homocomplex concomitant with signaling action when expressed in Huh7 cells (T.S. and M.G., unpublished observations). Thus, multimerization is a common feature for RIG-I and MDA5 signaling.

RIG-I has been shown to discriminate between RNA substrates wherein RNA containing a free 5′ triphosphate end, including purified influenza virus RNA, is selectively bound over RNA lacking free 5′ phosphates (18, 19). RNA transcribed *in vitro*, including the HCV RNA used in our study, contains 5′ triphosphate. It is notable that the HCV ss1 RNA is nonstructured (14) and did not bind efficiently to RIG-I, whereas 5′ or 3′ HCV NTR RNA did bind. Because the latter contains extensive secondary structure (14), it is likely that RIG-I discriminates self from nonself RNA by a combination of 5′ triphosphate and dsRNA motif recognition. We found that the RIG-I helicase domain and RD together form the functional unit that is sufficient to bind RNA, and that RIG-I and LGP2 bind HCV RNA. Relevance to this is supported by crystal structure analyses of DExD/H-box RNA helicase family members, in which interdependent interactions between helicase motifs I, II, and VI are necessary for ATP binding and hydrolysis, whereas motifs Ia and IV participate in oligonucleotide substrate binding (15). Thus, during virus infection, binding of dsRNA ligand could be expected to impose conformation changes that reposition the RD. This idea is supported by our trypsin digestion studies that identified a protease-resistant conformation change of the C terminus when RIG-I was bound to dsRNA and AMP-PNP. Our data indicate that the RD alone is a functional domain that, when expressed in trans, can mediate additional interdependent interactions with the RIG-I CARDs and the linker region between helicase motifs III and IV (amino acids 420–627) in which the latter interaction is essential for signaling inhibition. These results imply that the RD autoregulates RIG-I through internal interactions that control self-association.

Our results support a model of RIG-I autoregulation and signaling (Fig. 4*D*). This model predicts that, in resting cells, the RD mediates conformational constraints that, through internal interactions, maintain RIG-I in a orientation that masks the CARDs from signaling. During virus infection, RIG-I activation and signaling will then occur in steps involving dsRNA binding and conformation changes that stimulate self-association and that possibly involve ATP hydrolysis to displace the RD and unmask the CARDs for signaling through IPS-1 interaction. During the IFN response, increased levels of RIG-I may further promote its self-association and potentiate signaling to drive an IFN amplification loop. This model reflects the observed complex between the RD with RIG-I amino acids 1–228 encoding the tandem CARDs and is consistent with autoregulation of other CARD proteins, including Apaf-1 and NOD1. In each case, autoregulation by the C-terminal WD-40 and leucine-rich region (LRR) controls CARD signaling of caspase 9 by Apaf-1 and NF-κB activation by NOD1, respectively. Thus, the WD-40 or LRR function as the RD equivalent to control self-association and signaling, and deletion of each renders a constitutively active molecule (20, 21). This model reveals a common theme in CARD protein regulation, in which protein function is regulated by ligand binding-induced conformation changes that alter the RD or C-terminal motif to control oligmerization and signaling.

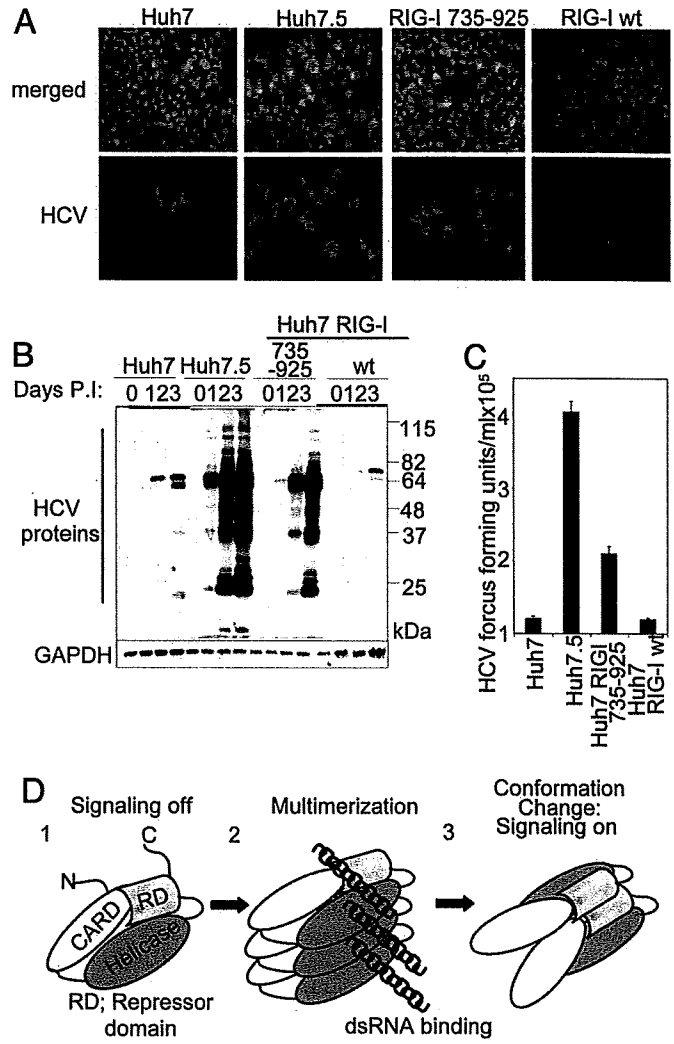

Fig. 4. The RD regulates cell permissiveness to HCV. Huh7, Huh7.5, Huh RIG-I wt, or Huh7-RIG-I-735–925 cells were infected with JFH-1 HCV 2A at a multiplicity of infection of 0.5. (*A*) After 48 h, cells were immunostained with HCV 2A antiserum (green). Nuclei were visualized by staining the cells with DAPI (blue). (*B*) Anti-HCV (*Upper*) and GAPDH immunoblot (*Lower*) of extracts from mock-infected cells (0) or from cells infected with JFH1 for 1, 2, or 3 days as indicated. The positions of HCV proteins are shown and have been defined previously (10). (*C*) Titer of HCV in supernatants collected from the indicated cell cultures 48 h after infection. (*D*) Model of RIG-I autoregulation and activation by virus infection. The RIG-I CARDs and domains encoding the helicase region and the RD are indicated.

We also identified an RD within the C terminus of LGP2. The LGP2 RD was necessary and sufficient for inhibition of RIG-I, but not MDA5, signaling despite being able to form a complex with either protein. Thus, LGP2 complex formation with MDA5 is not sufficient for signaling inhibition, possibly reflecting a unique cofactor or sequence differences of RIG-I and MDA5 control. We note that the MDA5 C-terminal region does not function as an RD. This lack of RD function and inhibitory control by LGP2 allows MDA5 to signal constitutively when expressed in abundance and could reflect an important role for MDA5 in amplifying IFN production and in the host response. We found that LGP2 blocked signaling by WT RIG-I but not RIG-I 1–228 in Huh7 cells, and the former occurred concomitant with disruption of WT RIG-I complex formation. In other work, LGP2 blocked signaling by RIG-I 1–228 when expressed in HEK 293 cells (22). This discrepancy could reflect cell-specific differences in the RIG-I pathways or

disparate assay conditions among studies. Our results indicate that LGP2 inhibits RIG-I through RD interactions that block RIG-I self-association, possibly by disrupting homotypic CARD/helicase domain and/or C terminus interactions. We also found that LGP2 binds to dsRNA and HCV RNA, thus implicating HCV dsRNA motifs as PAMP ligands of RIG-I and LGP2. Our studies indicate that RIG-I signaling inhibition is mediated directly by the LGP2 RD and possibly indirectly through sequestration of RNA substrates (2, 23). Moreover, LGP2 has been shown to block RIG-I signaling by disrupting assembly of a signaling complex on IPS-1 (22). Thus, LGP2 may influence the RIG-I pathway at multiple levels. As an IFN-stimulated gene, LGP2 expression is induced as a result of RIG-I signaling, and inhibition of RIG-I by LGP2 may provide a mechanism of feedback control to overall limit host response toxicity.

Huh7 cells expressing the RIG-I RD alone failed to induce the IFN-β promoter upon SenV infection, and they exhibited enhanced permissiveness for HCV. Our results affirm the role of RIG-I as a PRR of HCV and define the RD as a key modulator of host defenses that control HCV infection and production. Viral and therapeutic regulation of RD function could have implications for the modulation of immunity by directly regulating RIG-I signaling actions and IFN defenses.

Materials and Methods

Cell Culture and Viruses. Huh7 cells, Huh7.5 cells, and MEFs from WT, RIG-I-null, or MDA5-null cells, and their culture methods, have been described in refs. 6, 16, 24, and 25. Stable Huh7 cell lines harboring vector alone (Huh7v), or expressing the RIG-I RD (Huh7-RIG-I-735–925) or WT RIG-I (Huh7-RIG-I-wt), were produced by transfecting Huh7 cells with pCDNA3.1-hygro (Invitrogen, Carlsbad, CA) alone or in combination with pEFTak encoding RIG-I 735–925 or WT RIG-I, respectively. Cell clones were selected for resistance to hygromycine. Sendai virus (SenV; Cantell strain) was obtained from Charles River Laboratories (Wilmington, MA). HCV was produced from the RNA made from the pJFH-1 HCV 2a infectious clone, exactly as described in ref. 10. Virus infections and titrations were conducted and quantified as described in ref. 10.

Plasmids, Transfection, and Protein Analysis. For protein expression, we prepared modified pEF and pcDNA3.1 expression vectors (Invitrogen) pEFTak-Flag and pcDNA3.1-Myc, encoding amino-terminal tandem Flag or Myc epitopes, respectively. cDNA encoding the complete ORF of RIG-I, MDA5, or LGP2 was isolated by PCR from total cellular RNA and cloned into the pEFTak-Flag or pcDNA3.1-Myc by using standard methods. Mutant RIG-I, MDA5, or LGP2 expression constructs were prepared by using a PCR strategy or the Quickchange site-directed mutagenesis kit (Stratagene, La Jolla, CA). Primer sequences are available upon request. pIFN-β-luc, pCMV-*Renilla*-luc, and pPRDII-luc have been described previously (11, 12). Transfection, promoter-luciferase assay, immunoblot assay, and immunostaining and microscopy were conducted exactly as described in ref. 11.

Recombinant RIG-I was produced as a GST-RIG-I fusion by using baculovirus and High Five cells. GST-RIG-I was bound to glutathione Sepharose (Amersham Pharmacia Biosciences, Piscataway, NJ), then RIG-I was eluted by thrombin digestion and excess thrombin was eluted by passing through a benzamidine Sepharose column. RIG-I was then purified by Q Sepharose chromatography.

RNA Methods. RNA was synthesized from plasmids by using the T7 Megascript kit (Ambion, Austin, TX) in accordance with the manufacturer's protocol. JFH1 RNA, and HCV 5′ and 3′ NTR RNA, were produced from PCR products, made from the pJFH1 clone or HCV-N cDNA, respectively (26), by using a 5′ primer containing the T7 promoter. HCV ss1 RNA was transcribed from pCDNA3.1 HCV 1b NS3/4A (11). Biotinylated HCV RNA was transcribed and purified by using the AmpliScribe Flash transcription kit (Epicentre, Madison, WI) and Biotin-16-uridine-5′-triphosphate (Roche Diagnostics, Indianapolis, IN). For RNA-binding assay, biotinylated RNAs (1 μg) were incubated for 1 h at 25°C with 10 μg of protein from the cytoplasmic fraction of cells that were transfected with pEFTak-Flag expressing RIG-I, MDA5, or LGP2. The mixture was transferred into 400 μl of dialysis buffer containing 25 μl of streptavidin agarose affinity gel (Sigma, St. Louis, MO), rocked at 4°C for 2 h, collected by centrifugation, washed three times, resuspended in SDS sample buffer, incubated in a boiling bath for 5 min, and analyzed by SDS/PAGE and immunoblotting. For pIC, agarose pull-down assays were conducted as described in ref. 6.

Other Materials and Methods. Antibodies and additional molecular biology reagents are described in *SI Materials and Methods*.

We thank G. Sen (Cleveland Clinic Foundation, Cleveland, OH), M. David (University of California at San Diego, La Jolla, CA), T. Wakita (National Institutes of Infectious Diseases, Tokyo, Japan), and L. Gitlin and M. Colona (Washington University, St. Louis, MO) for reagents. This work was supported by National Institutes of Health Grants R01AI060389 and U19AI040035 Project 4, the Burroughs–Wellcome Fund, and a gift from Mr. and Mrs. R. Batcheldor (to M.G.).

1. Meylan E, Tschopp J, Karin M (2006) *Nature* 442:39–44.
2. Yoneyama M, Kikuchi M, Natsukawa T, Shinobu N, Imaizumi T, Miyagishi M, Taira K, Akira S, Fujita T (2004) *Nat Immunol* 5:730–737.
3. Kang DC, Gopalkrishnan RV, Wu Q, Jankowsky E, Pyle AM, Fisher PB (2002) *Proc Natl Acad Sci USA* 99:637–642.
4. Yoneyama M, Kikuchi M, Matsumoto K, Imaizumi T, Miyagishi M, Taira K, Foy E, Loo YM, Gale M, Jr, Akira S, *et al.* (2005) *J Immunol* 175:2851–2858.
5. Kato H, Takeuchi O, Sato S, Yoneyama M, Yamamoto M, Matsui K, Uematsu S, Jung A, Kawai T, Ishii KJ, *et al.* (2006) *Nature* 441:101–105.
6. Sumpter R, Loo Y-M, Foy E, Li K, Yoneyama M, Fujita T, Lemon SM, Gale M, Jr (2005) *J Virol* 79:2689–2699.
7. Kawai T, Takahashi K, Sato S, Coban C, Kumar H, Kato H, Ishii KJ, Takeuchi O, Akira S (2005) *Nat Immunol* 6:981–988.
8. Johnson CL, Gale M, Jr (2006) *Trends Immunol* 27:1–4.
9. Cui Y, Li M, Walton KD, Sun K, Hanover JA, Furth PA, Hennighausen L (2001) *Genomics* 78:129–134.
10. Loo YM, Owen DM, Li K, Erickson AK, Johnson CL, Fish PM, Carney DS, Wang T, Ishida H, Yoneyama M, *et al.* (2006) *Proc Natl Acad Sci USA* 103:6001–6006.
11. Foy E, Li K, Wang C, Sumpter R, Ikeda M, Lemon SM, Gale M, Jr (2003) *Science* 300:1145–1148.
12. Foy E, Li K, Sumpter R, Jr, Loo YM, Johnson CL, Wang C, Fish PM, Yoneyama M, Fujita T, Lemon SM, Gale M, Jr (2005) *Proc Natl Acad Sci USA* 102:2986–2991.
13. Kolumam GA, Thomas S, Thompson LJ, Sprent J, Murali-Krishna K (2005) *J Exp Med* 202:637–650.
14. Simmonds P, Tuplin A, Evans DJ (2004) *RNA* 10:1337–1351.
15. Caruthers JM, McKay DB (2002) *Curr Opin Struct Biol* 12:123–133.
16. Blight KJ, McKeating JA, Rice CM (2002) *J Virol* 76:13001–13014.
17. Wakita T, Pietschmann T, Kato T, Date T, Miyamoto M, Zhao Z, Murthy K, Habermann A, Krausslich HG, Mizokami M, *et al.* (2005) *Nat Med* 11:791–796.
18. Hornung V, Ellegast J, Kim S, Brzozka K, Jung A, Kato H, Poeck H, Akira S, Conzelmann KK, Schlee M, *et al.* (2006) *Science* 314:994–997.
19. Pichlmair A, Schulz O, Tan CP, Naslund TI, Liljestrom P, Weber F, Reis e Sousa C (2006) *Science* 314:997–1001.
20. Inohara N, Koseki T, del Peso L, Hu Y, Yee C, Chen S, Carrio R, Merino J, Liu D, Ni J, Nunez G (1999) *J Biol Chem* 274:14560–14567.
21. Hu Y, Ding L, Spencer DM, Nunez G (1998) *J Biol Chem* 273:33489–33494.
22. Komuro A, Horvath CM (2006) *J Virol* 80:12332–12342.
23. Rothenfusser S, Goutagny N, DiPerna G, Gong M, Monks BG, Schoenemeyer A, Yamamoto M, Akira S, Fitzgerald KA (2005) *J Immunol* 175:5260–5268.
24. Kato H, Sato S, Yoneyama M, Yamamoto M, Uematsu S, Matsui K, Tsujimura T, Takeda K, Fujita T, Takeuchi O, Akira S (2005) *Immunity* 23:19–28.
25. Gitlin L, Barchet W, Gilfillan S, Cella M, Beutler B, Flavell RA, Diamond MS, Colonna M (2006) *Proc Natl Acad Sci USA* 103:8459–8464.
26. Beard MR, Abell G, Honda M, Carroll A, Gartland M, Clarke B, Suzuki K, Lanford R, Sangar DV, Lemon SM (1999) *Hepatology* 30:316–324.

Negative regulation of the RIG-I signaling by the ubiquitin ligase RNF125

Kei-ichiro Arimoto*, Hitoshi Takahashi*, Takayuki Hishiki*, Hideyuki Konishi*, Takashi Fujita†, and Kunitada Shimotohno*‡

*Department of Viral Oncology and †Department of Genetic and Molecular Biology, Institute for Virus Research, Kyoto University, Sakyo-ku, Kyoto 606-8507, Japan

Edited by Tak Wah Mak, University of Toronto, Toronto, ON, Canada, and approved March 16, 2007 (received for review December 25, 2006)

Retinoic acid-inducible gene I (*RIG-I*) plays a pivotal role in the regulation of cytokine production induced by pathogens. The RIG-I also augments the production of IFN and other cytokines via an amplification circuit. Because the production of cytokines is closely controlled, up- and down-regulation of RIG-I signaling also needs strict regulation. The mechanism of this regulation, however, remains elusive. Here, we found that RIG-I undergoes proteasomal degradation after conjugation to ubiquitin by RNF125. Further, RNF125 conjugates ubiquitin to MDA5, a family protein of RIG-I as well as IPS-1, which is also a downstream protein of RIG-I signaling that results in suppressing the functions of these proteins. Because RNF125 is enhanced by IFN, these functions constitute a negative regulatory loop circuit for IFN production.

innate immunity | signal transduction

Upon viral infection, host cells activate the innate immune signaling cascades critical for effective antiviral immune responses (1, 2). The viral components, such as viral DNA or RNA, are recognized by Toll-like receptors (TLRs) that stimulate the production of antiviral factors including cytokines and induce inflammatory and adaptive immune responses (1–8). In addition to TLR-dependent activation of innate immunity, retinoic acid-inducible gene I (*RIG-I*) and other proteins in this family can also detect viral components or dsRNA, inducing the production of cytokines necessary to activate innate and adaptive immune responses (9, 10). The RIG-I is a DExD/H box RNA helicase with two caspase-recruiting domain (CARD)-like sequences and a helicase domain that is required for its interaction with dsRNA. The CARD-like domains are responsible for activating downstream signaling (9) through interactions with IPS-1/MAVS/VISA/Cardif (11–13).

The rapid induction of type-1 IFN expression is the key event in the initiation of the innate antiviral response, and it requires the pathogen-inducible activation of transcription factors that function synergistically to induce gene expression (9, 14–16). Among members of the IFN regulatory factor family, IRF3 and IRF7 play essential roles in virus-induced type-1 IFN gene activation after infection (9, 13, 17, 18).

Activation of TLRs results in a proinflammatory response necessary to prevent the spread of infection. Limiting TLR signaling, however, is essential to prevent this protective response from causing injury to the host. Several regulatory mechanisms that suppress TLR signaling have been described in earlier reports (19–22). Regulation of the TLR-independent, RIG-I-mediated signaling pathway regulating IRF3; however, it is not well understood. Recently, A20, an NF-κB-inducible ubiquitin-editing protein able to inhibit TLR3- and Sendai virus-induced activation of the ISRE promoter (23) was shown to inhibit this signaling pathway (24).

To clarify the mechanisms underlying the negative regulation of RIG-I signaling, we searched for a Ubl E3 ligase that modifies RIG-I. The result of the search was the identification of RNF125 (*Homo sapiens* ring-finger protein 125, GenBank accession no. NM_017831), also named TRAC-1 (T cell RING protein identified in activation screen), an E3 ubiquitin ligase serving a positive regulatory role in T cell activation (25), that functioned as an E3 ligase for RIG-I ubiquitin conjugation. Ubiquitin-conjugated RIG-I was degraded in a proteasome-dependent manner. We also observed that RNF125 possessed the ability to conjugate ubiquitin to MDA5, a member of the RIG-I protein family, as well as IPS1/MAVS/VISA/Cardif (referred to as IPS1 hereafter), a protein downstream of RIG-I signaling, which also suppresses RIG-I mediated signaling.

Results

Isolation of RNF125 as an Interacting Protein with UbcH8. RIG-I is reported to be conjugated (ISGylated) to ISG15 (26). UBE1L and UbcH8 function as E1 and E2 enzymes for ISGylation, respectively. Cotransfection of 293FT cells with plasmids encoding UBE1L, UbcH8, and ISG15 promoted the ISGylation of RIG-I (data not shown). The UbcH8 functions as an E2 enzyme for both ubiquitin and ISG15 conjugation (16, 27–33). We made an attempt to isolate a candidate E3-ligase capable of conjugating ISG15 or ubiquitin to RIG-I. We hypothesized that this candidate E3-ligase would interact with UbcH8 because, under certain circumstances, the interaction of E2 enzymes and E3 ligases can be observed *in vitro* during the conjugation of ubiquitin-like protein (Ubl) (32, 34). Using a yeast-two hybrid screening, we isolated RNF125 as an interacting protein with UbcH8. RNF125, a RING motif containing proteins, can act as a ubiquitin E3 ligase (25). A schematic diagram of RNF125 and its mutants used in this paper are shown in Fig. 1*a*. We found that RIG-I interacted with RNF125 as well as UbcH8 (Fig. 1 *c* and *d*). We analyzed the regions of RIG-I interacting with RNF125 by using deletion mutants of RIG-I as well as the region of RNF125 interacting with RIG-I (Fig. 1 *e* and *f*). From this analysis, the CARD domain of RIG-I as well as the C-terminal region of RIG-I were found to interact with the N-terminal region of RNF125.

RNF125 Is an E3-Ligase for Conjugation of Ubiquitin to RIG-I. We analyzed whether the E3-ligase activity of RNF125 is responsible for the ubiquitination of RIG-I. When FLAG-RIG-I, HA-RNF125, and Myc-Ub were expressed in 293FT cells, ubiquitin conjugation to RIG-I was observed (Fig. 2*a*). The level of ubiquitination was low in the absence of ectopic RNF125 expression. The fact that RNF125 is the ubiquitin E3-ligase for

Author contributions: K.-i.A. and K.S. designed research; K.-i.A. and H.K. performed research; H.T., T.H., and T.F. contributed new reagents/analytic tools; K.-i.A., H.T., T.H., H.K., and K.S. analyzed data; and K.-i.A. and K.S. wrote the paper.

The authors declare no conflict of interest.

This article is a PNAS Direct Submission.

Abbreviations: CARD, caspase-recruiting domain; CHX, cycloheximide; MEF, mouse embryonic fibroblast; TLR, Toll-like receptor.

‡To whom correspondence should be addressed. E-mail: kshimoto@virus.kyoto-u.ac.jp.

This article contains supporting information online at www.pnas.org/cgi/content/full/0611551104/DC1.

www.pnas.org/cgi/doi/10.1073/pnas.0611551104

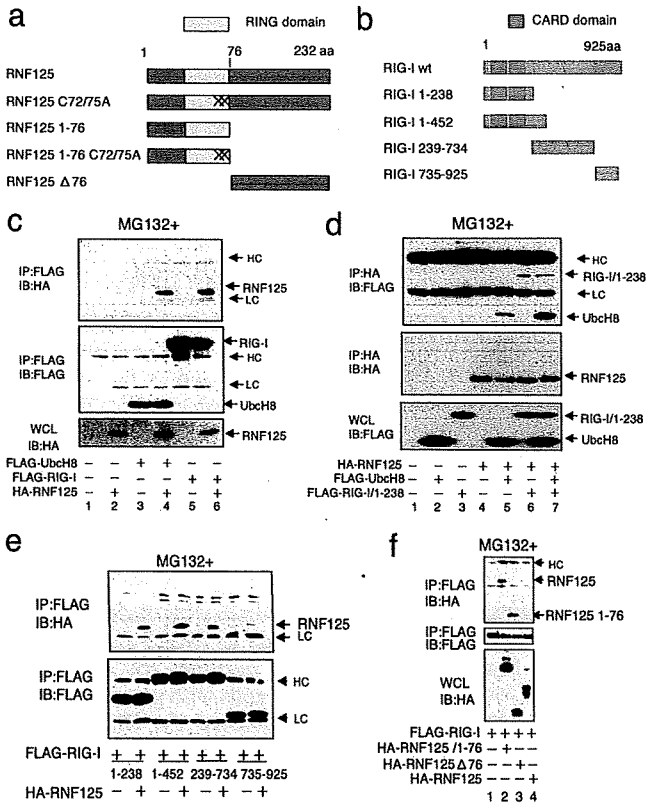

Fig. 1. Association of RNF125 with UbcH8 and RIG-I. (*a* and *b*) Schematic structure of RNF125, RIG-I, and their derivatives used in this work. "X" indicates site of cysteine residue substitution with alanine at the 72nd and 75th residues in RNF125. (*c* and *d*) Coimmunoprecipitation experiments. The 293FT cells were transfected as indicated. Thirty-six hours after transfection, protein associations were analyzed either by coimmunoprecipitation using anti-FLAG antibody, followed by Western blot using anti-HA antibody (*c*), or by coimmunoprecipitation using anti-HA antibody, followed by anti-FLAG antibody (*d*). (*e*) Analysis of the RIG-I domain that interacts with RNF125. Plasmids expressing various deletion mutants, including amino acids 1–238, 1–452, 239–734, and 735–925 of RIG-I fused to a FLAG epitope tag (*b*), were transfected into 293FT cells with or without a plasmid encoding HA-RNF125. Complex formation was examined by immunoprecipitation with an anti-FLAG antibody followed by immunoblotting using the anti-HA antibody (*Upper*). The amount of each RIG-I mutant in the complex is indicated (*Lower*). (*f*) Analysis of the association of RIG-I with RNF125 mutants. Plasmids as indicated were transfected into 293FT cells. The lysates were immunoprecipitated by using an anti-FLAG antibody, followed by blotting with the anti-HA antibody (*Top*). The quantity of FLAG-RIG-I in the immunocomplexes as well as the RNF125 and mutants in whole-cell lysates are also shown in *Middle* and *Bottom*, respectively. HC and LC indicate the heavy and light chains of human immunoglobulins, which are also indicated in the following figures. All cells in *c–f* were treated with MG132.

RIG-I was further confirmed by the suppression of endogenous RNF125 using siRNA. Transfection of cells with siRNF125–3 strongly suppressed the production of RNF125 mRNA, leading to a substantial reduction in RNF125 protein levels in 293FT cells (Fig. 2*b Upper*). In cells treated with siRNF125–3, with the exception of those treated with control siRNA, the levels of RIG-I polyubiquitination were substantially reduced (Fig. 2*b Lower*).

Analysis of the E3-Ligase Domain of RNF125 and a Target Region in RIG-I for Ubiquitination. To verify the role of the RNF125 RING domain in ubiquitin conjugation to RIG-I, we performed a mutational analysis. Although RIG-I could be conjugated to ubiquitin by WT RNF125 (Fig. 2*a*, lane 3), an RNF125 mutant [in which the 72nd and 75th cysteine residues were substituted with alanine (C72/75A)] was unable to mediate RIG-I ubiquitination (Fig. 2*a*, lane 4). A peptide encompassing the first 76 residues of RNF125 (1–76 aa), a region containing the intact RING domain, mediated ubiquitin conjugation similar to the WT RNF125. The mutant Cys-72 and Cys-75 in this peptide (1–76 aa C72/75A), however, completely abrogated its ubiquitin-conjugating activity (Fig. 2*a*, lane 6).

To verify the region of RIG-I conjugated to ubiquitin, we analyzed ubiquitin conjugation to FLAG-RIG-I mutants in cells coproducing HA-RNF125 and Myc-Ub (Fig. 2*c*). Peptides containing CARD domain of RIG-I, amino acids 1–238 (RIG-1/1–238) or 1–452 (RIG-I/1–452), were ubiquitinated at higher levels than intact RIG-I. In contrast, C-terminal RIG-I peptides, RIG-I/239–734 and RIG-I/735–925, were only weakly conjugated. Using the N-terminal region of RIG-I (RIG-I/1–238) as a substrate, we confirmed that RNF125, and not Efp (estrogen-responsive finger proteins), another ubiquitin E3 ligase, efficiently conjugated ubiquitin (data not shown), further supporting the conclusion that RNF125 acts as an E3 ligase for RIG-I.

Degradation of RIG-I Is Enhanced by the Expression of RNF125. Polyubiquitin was primarily conjugated to the N-terminal CARD-containing region of RIG-I (Fig. 2*c*). Steady-state levels of the ubiquitin-conjugated peptide containing the N-terminal region, RIG-I/1–238, were increased in cells treated with MG132, a proteasome inhibitor (Fig. 2*d*). These results suggest that RNF125-dependent RIG-I ubiquitination precedes proteasome-dependent degradation. Full-length RIG-I was also degraded with ectopic expression of RNF125 but not with the mutant C72/75A in 293FT cells (Fig. 2*e*). The levels of RIG-I were reduced as increasing amounts of RNF125 were expressed (Fig. 2*f*). Under these conditions, mRNA levels of RIG-I, GAPDH, p53, and tubulin remained unchanged. When cells were treated with MG132, the degradation of RIG-I was suppressed. These results clearly demonstrate that RNF125 acts as a ubiquitin E3-ligase regulating the cellular levels of RIG-I through proteasomal degradation. Proteasomal degradation of RIG-I was also observed in other cell types such as HeLa and HepG2 (data not shown).

Degradation of RIG-I is enhanced by the presence of RNF125. The level of RIG-I was reduced after addition of cycloheximide (CHX), when RNF125 was ectopically expressed, but no such reduction in RIG-I was observed in cells without ectopic expression of RNF125 (Fig. 2*g Upper*). Such degradation of RIG-I in cells treated with poly I:C was not observed in cells expressing RNF125 specific siRNA, siRNA125–3, although substantial amount of RIG-I degradation in cells treated with control siRNA could be observed (Fig. 2*g*).

E2 Enzymes Involved in Ubiquitin Conjugation to RIG-I. RNF125 interacts with several E2 enzymes (25), and one of these enzymes most likely acts as an E2 for ubiquitin conjugation to RIG-I. To identify the E2 acting upstream of RNF125 in RIG-I conjugation, we performed an *in vitro* assay examining ubiquitin conjugation to RIG-I [see supporting information (SI) Fig. 6]. We identified that UbcH1, UbcH5a, UbcH5b, and UbcH5c functioned as an E2 enzyme. The enzymes UbcH1 and UbcH5a-c conjugated ubiquitin to RNF125 and RIG-I via K48 (data not shown).

Further, by analyzing ubiquitin conjugation to RIG-I in 293FT cells by ectopic expression of the E2 enzymes, we observed only UbcH5c, and not other E2 enzymes, showing enhanced ubiquitin conjugation to RIG-I, suggesting that UbcH5c is the major E2 enzyme functioning *in vivo* (data not shown).

Expression of RNF125 Suppresses the Activation of IRF3. The ability of RNF125 to modulate RIG-I protein levels suggests that

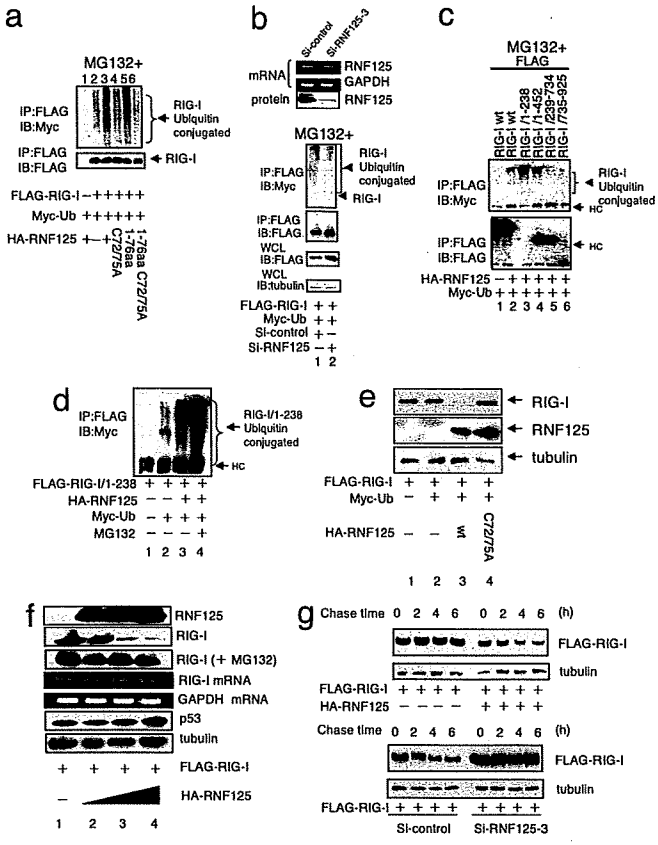

Fig. 2. Ubiquitin conjugation to RIG-I. (*a*) Ubiquitin conjugation to RIG-I by WT and mutant RNF125. Plasmids encoding FLAG-RIG-I and Myc-Ub were cotransfected into 292FT cells with a plasmid encoding either WT or mutant RNF125. The RIG-I ubiquitination was monitored by immunoprecipitation. All cells were treated with MG132. (*b*) Inhibition of RIG-I ubiquitin conjugation after suppression of endogenous RNF125. The siRNF125–3, an siRNA that down-regulates RNF125 mRNA, or a control siRNA were transfected into the 293FT cells. The mRNA and protein levels of RNF125 were monitored by RT-PCR or Western blot, respectively, 36 h after transfection (*Upper*). The 293FT cells transfected with plasmids encoding FLAG-RIG-I and Myc-Ub were simultaneously treated with control siRNA or siRNF125–3; RIG-I ubiquitination in cell lysates was then analyzed by coimmunoprecipitation. All cells were treated with MG132. The quantity of RIG-I present in the immunoprecipitants was monitored by immunoblot with an anti-FLAG antibody. The total RIG-I present in an aliquot of whole-cell lysate is also shown. Tubulin serves as the control in this analysis (*Lower*). (*c*) Analysis of the region for ubiquitin conjugation in RIG-I. Plasmids encoding HA-RNF125 and Myc-Ub were cotransfected into 293FT cells with WT or deletion mutants of FLAG-RIG-I. We analyzed cell lysates harvested 36 h after transfection for interactions between RNF125 and WT or mutant RIG-I by immunoprecipitation (note that the expression level of 1–238 was very low; despite the low levels, however, the interaction with RIG-I was clearly observed). All cells were treated with MG132. (*d*) Ubiquitin conjugation stimulates RIG-I degradation in a proteasome-dependent manner. Plasmids encoding a FLAG-tagged version of the RIG-I N terminus, FLAG-RIG-I/1–238, HA-RNF125, and Myc-Ub were transfected into 293FT cells as indicated. After culturing with or without MG132, the levels of ubiquitination were analyzed by immunoprecipitation. (*e*) RNF125 stimulates RIG-I degradation. Plasmids encoding FLAG-RIG-I and Myc-Ub were cotransfected into 293FT cells with WT or a point mutant of HA-RNF125. Cells were harvested 36 h after transfection and were analyzed for proteins by Western blot. (*f*) RIG-I was degraded by RNF125 in a dose-dependent manner. The 293FT cells were transfected with a plasmid encoding FLAG-RIG-I (0.5 μg) and varying doses of a plasmid encoding HA-RNF125 (0, 0.5, 1, and 2 μg). Half of each cell aliquot was treated with MG132. The levels of both RIG-I mRNA and protein were examined in cells harvested 48 h after transfection. "RIG-I (+MG132)" indicates analysis of the RIG-I protein in cells treated with MG132. As a control, the cellular proteins p53 and tubulin and GAPDH mRNA analyses are shown. (*g*) RIG-I was degraded by ectopic and endogenous RNF125. A plasmid encoding FLAG-RIG-I with or without a plasmid encoding HA-RNF125 was transfected into 293FT cells. Thirty-six hours after transfection, the cells were treated with CHX (final concentration, 50 μg/ml), and were analyzed by Western blot (*Upper*). Plasmids encoding FLAG-RIG-I and RNA for si-control or siRNF125–3 were transfected into 293FT cells. Twenty-four hours after transfection, these cells were treated with Poly I:C for 12 h, followed by addition of CHX. Cells were harvested at the indicated times after addition of CHX and analyzed by Western blot (*Lower*).

RNF125 may play an important role in the regulation of IRF3 activity. We analyzed this possibility by using a luciferase reporter gene driven by the IFNβ promoter, IFNβ-luc, to examine the effect of RNF125 on IRF3 activity after stimulation with poly I:C or Sendai virus infection (Fig. 3*a*). The 293FT cells expressing IFNβ-Luc, RIG-I, and RNF125 were treated with poly I:C or Sendai virus infection. We observed a marginal increase in luciferase activity in those cells lacking ectopic RIG-I and RNF125 expression (Fig. 3*a*, lanes 1–3). Luciferase activity was enhanced by the ectopic expression of RIG-I alone and further augmented by treatment with poly I:C or Sendai virus (Fig. 3*a*, lanes 4–6). Cells expressing RNF125, however, exhibited reduced reporter activity, and this decreased in a dose-dependent manner (Fig. 3*a*, lanes 7–15). The enhanced luciferase activity seen after polyIC treatment or Sendai virus infection was almost completely abrogated by high levels of RNF125 expression (Fig. 3*a*, lanes 12 and 15). Suppressive activity of IFNβ-luc was not observed by the mutant RNF125 that lacks the conjugation activity and ability to interact with RIG-I (Fig. 3*b*). Furthermore, we observed that ectopic RNF125 expression inhibited nuclear localization of IRF3 by poly I:C treatment (SI Fig. 7).

We next examined the effect of endogenous RNF125 on IRF3 activation by knocking down RNF125 mRNA by using siRNA. The 293FT cells treated with siRNF125–3 were subsequently transfected with plasmids encoding IFNβ-luc and RIG-I. Cells were then infected with Sendai virus or mock infected. Sendai virus-induced luciferase activity was substantially greater in cells in which RNF125 expression was suppressed by siRNF125–3 (Fig. 3*c Left*, lanes 2 and 4). Additionally, endogenous IFNβ mRNA production was also increased in those cells (Fig. 3*c Right*).

To examine whether the ability of RNF125 to suppress IRF3 activation in 293FT cells was physiologically relevant, an experiment was performed by using primary mouse embryonic fibroblasts (MEFs). RIG-I signaling is essential for virus-induced cytokine secretion in conventional dendritic cells (DCs) and MEFs (35). The MEFs transfected with plasmids encoding mouse RNF125 (mRNF125) and IFNβ-luc were infected with Sendai virus or mock infected. Induced induction of luciferase activity was directly correlated with the degree of Sendai virus infection (Fig. 3*d*). However, the induced luciferase activity was strongly suppressed by the ectopic expression of mRNF125 (Fig. 3*d*, lanes 7–9). Furthermore, transfection of MEFs with siRNF125–3 led to reduced mRNF125, mRNA, and protein levels (data not shown) and somewhat enhanced luciferase production after Sendai virus infection (Fig. 3*e*).

We further confirmed the suppression of RIG-I signaling by RNF125 by examining the release of IFNβ in the culture medium. In cells treated with poly I:C as well as infected with Sendai virus, IFNβ released was significantly reduced by the expression of RNF125 in a dose-dependent manner (Fig. 3*f*). Furthermore, MEFs treated with si-RNF125–3 showed substantial increase of IFNβ release in the culture medium upon polyI:C and Sendai virus infection (Fig. 3*g*).

RNF125, UbcH5, and RIG-I Are Up-Regulated by IFN-α and Poly I:C. The production of proteins related to Ubl conjugation is often regulated by IFNs (36). Thus, the modification of RIG-I by ubiquitin is most likely regulated by the coordinated induction of

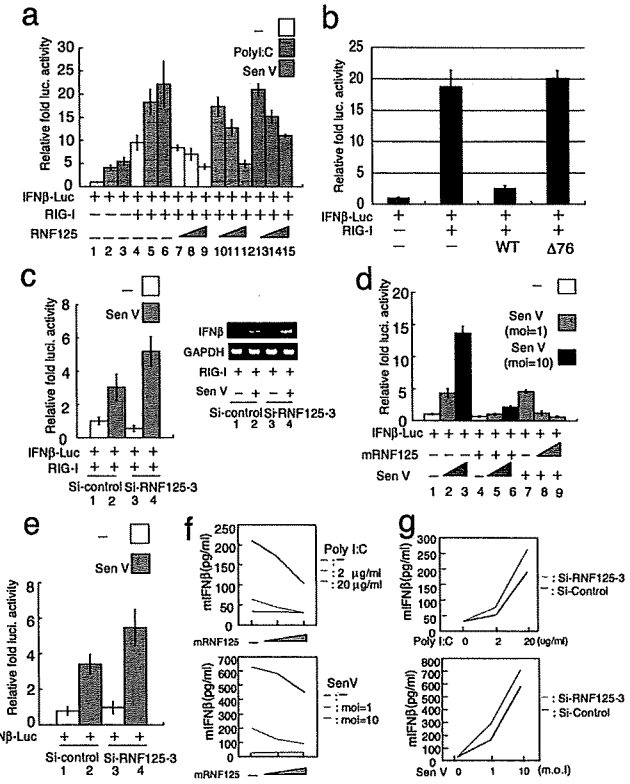

Fig. 3. Suppression of RIG-I function by ubiquitination. (*a*) The RNF125 suppressed the IFNβ-driven luciferase activity, activated by RIG-I (at the left). The 293FT cells were transfected with plasmids encoding RIG-I (50 ng) and IFNβ-luc (50 ng) with varying amounts of a plasmid encoding RNF125 (10, 50, and 100 ng). Twenty-four hours after transfection, cells were treated with polyIC (blue) or infected with Sendai virus (pink). Cells were harvested 12 h after the treatment; luciferase activity in the lysates was then measured. The RNF125 suppressed the production of IFNβ mRNA. (*b*) The 293FT cells transiently expressing IFNβ-luc, RIG-I, and RNF125WT or Δ76 were analyzed for luciferase activity 36 h after transfection. (*c*) Effect of siRNF125–3, a small inhibitory RNA specific for RNF125 mRNA, on IFNβ-luc activity and IFNβ level. The 293FT cells were transfected with plasmids encoding IFNβ-luc and RIG-I and treated with control siRNA or siRNF125–3. An aliquot of cells was then infected with Sendai virus. Twenty-four hours after infection, luciferase activity (*Left*) and IFNβ mRNA levels, assessed by RT-PCR (*Right*), were measured. (*d*) Effect of mouse RNF125 on endogenous RIG-I signaling in primary MEFs. The MEFs were transfected with plasmids encoding mouse RNF125 (100 ng in lanes 4, 5, 6, and 8 or 200 ng in lane 9) and IFNβ-luc (50 ng) in combination as indicated. Twelve hours after transfection, cells were infected with Sendai virus at the indicated multiplicity of infection (MOI) or mock infected. Luciferase activity in cell lysates prepared 24 h after treatment was measured. White box, mock infected; pink box, Sendai virus infected with MOI 1; black box, Sendai virus with MOI of 10. (*e*) The MEFs were transfected with plasmids encoding IFNβ-luc and treated with control siRNA or siRNF125–3 (final concentration of 8 nM). Cells were then infected with Sendai virus at MOI of 1. Twenty-four hours after infection, luciferase activity was measured. (*f*) The level of IFNβ in culture medium in cells was decreased in an RNF125 dose-dependent manner. Cells transfected with different amounts of plasmids encoding RNF125 were treated with 0 (green), 2 (pink), and 20 (blue) μg/ml of poly I:C (*Upper*) and with 0 (green), 1 (pink), and 10 MOI (blue) of Sendai virus (*Upper*). Twelve hours after the treatment, IFNβ in the culture medium was measured by ELISA system. (*g*) The level of IFNβ was increased in MEFs treated with siRNA for RNF125-specific mRNA. Cells treated with control siRNA (black bars) or siRNA125–3 (pink bars) were treated with different doses of poly I:C or Sendai virus infection and were analyzed for IFNβ in culture medium.

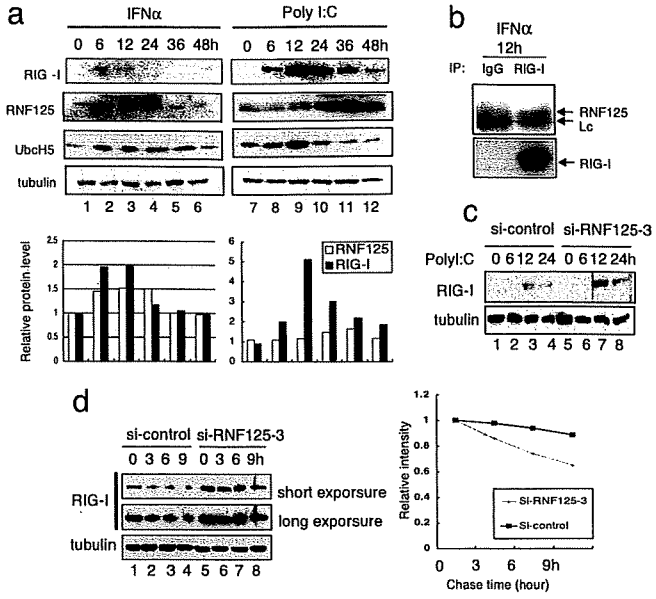

Fig. 4. Induction of RIG-I and the Ubls by IFNα or poly I:C treatment. (*a*) HepG2 cells were harvested at the indicated times after treatment with IFNα (10^3 units/ml) or Poly I:C (2 μg/ml) and were analyzed for protein levels by Western blot. As a control, the level of tubulin is shown. The protein level of each band is quantified and graphed. (*b*) Endogenous association of RIG-I and RNF125. Jurkat cells were incubated with IFNα (1,000 units/ml) and MG132 (final 10 μM). After 12 h, whole-cell lysates were subjected to immunoprecipitation assay using anti-RIG-I antibody or control antibody, followed by immunoblotting for detection of RNF125 and RIG-I. (*c*) Influence of siRNA specific to RNF125 for RIG-I levels. Cells treated with siRNA were further treated with poly I:C and then harvested at the indicated times after poly I:C treatment. The lysates were analyzed for the levels of endogenous RIG-I. Tubulin acts as a control. (*d*) HepG2 cells treated with siRNA were further treated with IFNα for 12 h and then harvested at the indicated times after CHX treatment. The lysates were analyzed for the levels of endogenous RIG-I. Tubulin acts as a control. The intensity of each band is quantified and graphed.

Ubl-conjugating proteins. We analyzed the levels of RIG-I, RNF125, and UbcH5 in HepG2 cells at various times after treatment with IFNα and poly I:C (Fig. 4a). Low levels of RNF125 were present before IFNα and Poly I:C treatment, but its expression peaked 12–36 h after induction. Although RIG-I was barely detectable at the time of induction, it became detectable at 6 h and peaked at 12 h. The decreases in RIG-I expression correlated temporally with the increases in RNF125 and UbcH5 (Fig. 4*a*), suggesting that RNF125 decreased the levels of RIG-I after IFN induction. Quantitative analysis indicated that RIG-I level showed reverse correlation of RNF125 (Fig. 4*a*, graph). The fact that constitutive association of endogenous RIG-I and RNF125 (Fig. 4*b*) supports the possibility that RNF125 conjugates ubiquitin to RIG-I to promote proteasomal degradation. We confirmed this hypothesis by treating cells with RNF125 siRNA. In cells treated with control siRNA, RIG-I expression increased at 12 and 24 h after poly I:C treatment, but, in cells treated with siRNF125–3, RIG-I expression was higher, and it sustained longer than treated control cells (Fig. 4*c*, compare lanes 3 and 7 and 4 and 8). To measure a half-life of RIG-I, we treated HepG2 cells expressing siRNA specific to RNF125 or control siRNA with IFNα for 12 h and then added CHX. Cells harvested at the indicated time after CHX treatment were analyzed for RIG-I by Western blot and quantified the intensity of the bands (Fig. 4*d*). Calculated half-life of RIG-I in cells treated with siRNA specific to RNF125 was 16 h and 8 h in cells treated with control siRNA.

RNF125 Exhibits Ubiquitin-Conjugating E3-Ligase Activity for MDA5 and IPS1. MDA5 is a member of the RIG-I protein family and contains CARD domain. The IPS1, a CARD-containing protein, downstream of RIG-I signaling interacts with RIG-I

IMMUNOLOGY

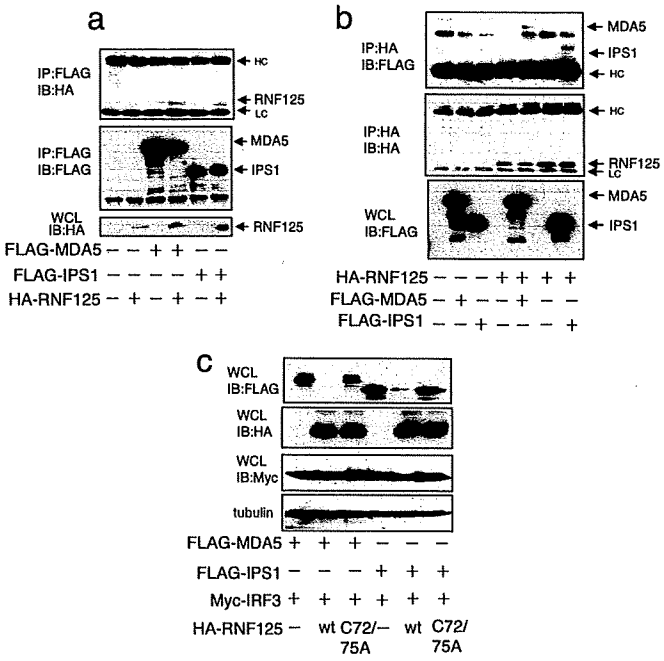

Fig. 5. Association of RNF125 with MDA5 and IPS-1. A plasmid encoding FLAG-MDA5 or FLAG-IPS1 was transfected into 293FT cells in the presence or absence of a plasmid encoding HA-RNF125. (*a* and *b*) Protein–protein interactions were monitored by coimmunoprecipitation using the anti-FLAG antibody, followed by Western blot with the anti-HA antibody (*a*) and coimmunoprecipitation using the anti-HA antibody, followed by Western blot with the anti-FLAG antibody (*b*). All cells were grown in medium containing MG132. (*c*) MDA5 and IPS1 were also degraded by RNF125. A plasmid encoding Myc-IRF3 and FLAG-MDA5 or FLAG-IPS1 were transfected into 293FT cells with or without a plasmid encoding HA-RNF125 or HA-RNF125 C72/75A. Thirty-six hours after transfection, cells were harvested and were analyzed for protein levels by Western blot.

through its CARD domain. These proteins are associated with RNF125 (Fig. 5 *a* and *b*). The concentrations of MDA5 and IPS1 were observed to reduce in cells expressing RNF125 ectopically (Fig. 5*c*). Furthermore, we noticed that these proteins were ubiquitin-conjugated by RNF125, and not by the RNF125 mutant, although the levels of conjugation differed between the substrates (SI Fig. 8 *a* and *b*). Suppression of conjugation of ubiquitin to these proteins was observed by treatment with siRNA specific to RNF125 (SI Fig. 8 *a* and *b Right*). Bringing all these data together, RNF125 serves as a ubiquitin E3-ligase for MDA5 and IPS1 as well as for RIG-I.

Analyzing a candidate E2 enzyme for ubiquitin conjugation to MDA5 and IPS1 by RNF125 in an *in vitro* assay, we observed that UbcH1 and UbcH5a-c were also involved in the process (SI Fig. 8*c*).

Signaling from MDA5 as Well as from IPS1 Was Suppressed by RNF125 Ubiquitin Conjugation-Dependent Manner. Effect of conjugation of ubiquitin to MDA5 and IPS1 by RNF125 on their downstream signaling was analyzed by luciferase assay. Cells were transfected with plasmids expressing IFNβ-luc, MDA5, or IPS1 together with that expressing RNF125 or its mutant. The luciferase activities in cells expressing MDA5 and IPS1 were severely impaired by the expression of RNF125, and not by Δ76 (SI Fig. 9 *a* and *b*). Alternatively, those cells treated with siRNF125–3 showed increased activity of luciferase in the cells bearing both MDA5 and IPS1 (SI Fig. 9 *a* and *b*). Luciferase activity driven by p53-binding promoter was not affected in cells expressing ectopic p53 and RNF125 (SI Fig. 9*c*).

Discussion

We demonstrated that RIG-I is ubiquitinated before its proteasome-dependent degradation. The RNF125 functioned as an E3-ligase for this conjugation process, because ectopic expression of RNF125 enhanced (Fig. 2*a*) and suppression of endogenous RNF125 by siRNA severely impaired the ubiquitin conjugation of RIG-I (Fig. 2*b*). The RNF125, a RING finger-containing protein (25), also known as TRAC-1, exerts a positive regulatory role on T cell activation. Expression of RNF125/TRAC-1 is higher in lymphoid tissues but is also expressed in a variety of other tissues. The role of RNF125 described here appears to be distinct from that previously reported.

It can be observed that the N-terminal region of RIG-I, the region containing the CARD domain, was conjugated to ubiquitin, by minimal incorporation of ubiquitin to the C-terminal half of RIG-I (Fig. 2*c*). Conjugation was enhanced after the deletion of the C-terminal portion of RIG-I, which contained the helicase domain, a result that is consistent with the earlier postulation that the C terminus of RIG-I may mask the function of the N-terminal region (9).

The MDA5, an RIG-I family member, and IPS1, the downstream signaling proteins that interact with RIG-I via the RIG-I CARD, interacted with RNF125 and were also ubiquitin conjugated (Fig. 5 *a* and *b* and SI Fig. 8 *a* and *b*). These results suggest that RNF125 is a ubiquitin E3-ligase with activity against proteins containing CARD domains. These two ubiquitin-conjugated proteins also underwent proteasomal degradation (Fig. 5*c*). We noticed that MDA5 was ubiquitin-conjugated less than RIG-I by RNF125, but the level of this proteins decreased substantially (Fig. 5*c*). We do not know the reason for this, but there may be the possibility that a small amount of ubiquitination to MDA5 may be sufficient to trigger the degradation or that there is a pathway other than ubiquitin-dependent proteasomal degradation for MDA5 degradation. These observations suggest that ubiquitination of RIG-I/MDA5 and IPS1 inhibits RIG-I signaling by shunting these proteins toward proteasomal degradation. Given that the production of cytokines affects a wide variety of responses in innate and acquired immunity, activation of RIG-I signaling by viral pathogens is quite likely to be strictly controlled. Suppression of endogenous RNF125 levels by siRNA enhanced luciferase activity driven by the IFNβ promoter and up-regulated IFNβ expression (Fig. 3*c*), which clearly demonstrates that RNF125 functions as a negative regulator of RIG-I signaling. Importantly, the negative regulatory function of RNF125 is inversely related to IFN signaling in cells, a factor most likely contributing to the down-regulation of IFN levels as the viral infection resolves.

The suppression of IRF3 signaling by RNF125 was not limited to cultured cell lines, but was also seen in primary MEFs (Fig. 3*d*), in which RIG-I is the primary factor activating IRF3 during RNA virus infection (35). These results clearly indicate that RNF125 plays an important role in suppressing RIG-I signaling in physiologically immunocompetent cells.

The IFNα and Poly I:C treatment transiently up-regulated RIG-I levels, which peaked at 12 h after the treatment of HepG2 cells (Fig. 4*a*). Reductions in RIG-I expression correlated with the induction of RNF125 and UbcH5, suggesting that these proteins may enhance the degradation of RIG-I by ubiquitin conjugation. This result is found to be consistent with the *in vitro* experiments (Fig. 2 *a* and *b*).

Materials and Methods

Cell Culture, Transfection, and Luciferase Reporter Assays. For details on cell culture, transfection, and luciferase reporter assays, see *SI Methods*.

Yeast Two-Hybrid Screening. Yeast two-hybrid screening was performed as described in *SI Methods*.

Construction of cDNA Expression Plasmids. Expression constructs for RIG-I, MDA5, and IPS-1 have been described (9). Plasmids expressing WT and mutant ubiquitin were obtained from K. Nakayama (Division of Cell Biology, Medical Institute of Bioregulation, Kyushu University, Fukuoka, Kyushu, Japan). WT RNF125 (amino acid 1–232) and mouse RNF125 were cloned into the pCAG vector. To generate point mutants, alanine was substituted for the targeted residues by PCR. The N- and C-terminal truncation mutants (RNF125 1–76 and RNF125Δ76) were generated by standard PCR. The RNF125 and RIG-I were cloned into the pGEX-6P-1 vector (Amersham, Piscataway, NJ) in-frame with an N-terminal GST.

siRNA and Measurement of mRNA. siRNA duplex sequences (siRNF125–3, 5′-CCGUGUGCCUUGAGGUGUU-3′) were custom synthesized by Proligo (Boulder, CO). A control nucleotide, si-control, was purchased from Dharmacon (Lafayette, CO) (nonspecific control duplex IV). mRNA was measured by RT-PCR.

Western Blotting and Immunoprecipitation. Western blotting and immunoprecipitation were done as reported in *SI Methods*.

ELISA. For details on ELISA, see *SI Methods*.

Antibodies and Reagents. Antibodies to FLAG (anti-Flag; M2), HA (12CA5) and HA (3F10) were purchased from Sigma (St. Louis, MO) and Roche (Indianapolis, IN), respectively. Anti-Myc (9E10), anti-IRF3 (FL425) antibody, and anti-ubiquitin antibodies were obtained from Santa Cruz Biotechnology (Santa Cruz, CA). Anti-UbcH5, which reacts with UbcH5a-c, and anti-α tubulin were acquired from Chemicon (Temecula, CA) and Oncogene Research Products (San Diego, CA), respectively. Anti-GST antibodies were purchased from Amersham. Anti-RNF125 polyclonal antibodies were generated in rabbits by using the RNF125 peptide from 215 to 232 aa. Anti-RIG-I monoclonal antibody was described (9). Anti-RIG-I polyclonal antibodies were generated in rabbits by using the RIG-I recombinant protein from 1 to 238 aa. CHX was purchased from Nacalai Tesque (Kyoto, Japan). Poly (I:C) and MG132 were purchased from Amersham and Peptide Institute (Osaka, Japan), respectively.

The GenBank accession number for mRNF125 is AB259692.

We thank Dr. K. I. Nakayama for providing the plasmids expressing the ubiquitin mutants. This work was supported by grants-in-aid for cancer research and for the second-term comprehensive 10-year strategy for cancer control from the Ministry of Health, Labour and Welfare as well as by Grant-in-Aid for Scientific Research on Priority Areas "Integrative Research Toward the Conquest of Cancer" from the Ministry of Education, Culture, Sports, Science and Technology of Japan.

1. Iwasaki A, Medzhitov R (2004) *Nat Immunol* 5:987–995.
2. Theofilopoulos AN, Baccala R, Beutler B, Kono DH (2005) *Annu Rev Immunol* 23:307–336.
3. Takeda K, Akira S (2005) *Int Immunol* 17:1–14.
4. Medzhitov R, Janeway CA, Jr (1997) *Cell* 91:295–298.
5. Janeway CA, Jr, Medzhitov R (2002) *Annu Rev Immunol* 20:197–216.
6. Akira S, Takeda K, Kaisho T (2001) *Nat Immunol* 2:675–680.
7. Takeda K, Kaisho T, Akira S (2003) *Annu Rev Immunol* 21:335–376.
8. Le Bon A, Tough DF (2002) *Curr Opin Immunol* 14:432–436.
9. Yoneyama M, Kikuchi M, Natsukawa T, Shinobu N, Imaizumi T, Miyagishi M, Taira K, Akira S, Fujita T (2004) *Nat Immunol* 5:730–737.
10. Andrejeva J, Childs KS, Young DF, Carlos TS, Stock N, Goodbourn S, Randall RE (2004) *Proc Natl Acad Sci USA* 101:17264–17269.
11. Kawai T, Takahashi K, Sato S, Coban C, Kumar H, Kato H, Ishii KJ, Takeuchi O, Akira S (2005) *Nat Immunol* 6:981–988.
12. Seth RB, Sun L, Ea CK, Chen ZJ (2005) *Cell* 122:669–682.
13. Meylan E, Curran J, Hofmann K, Moradpour D, Binder M, Bartenschlager R, Tschopp J (2005) *Nature* 437:1167–1172.
14. Malakhov MP, Kim KI, Malakhova OA, Jacobs BS, Borden EC, Zhang DE (2003) *J Biol Chem* 278:16608–16613.
15. Schwartz DC, Hochstrasser M (2003) *Trends Biochem Sci* 28:321–328.
16. Zhao C, Beaudenon SL, Kelley ML, Waddell MB, Yuan W, Schulman BA, Huibregtse JM, Krug RM (2004) *Proc Natl Acad Sci USA* 101:7578–7582.
17. Sumpter R, Jr, Loo YM, Foy E, Li K, Yoneyama M, Fujita T, Lemon SM, Gale M, Jr (2005) *J Virol* 79:2689–2699.
18. Morales FC, Takahashi Y, Kreimann EL, Georgescu MM (2004) *Proc Natl Acad Sci USA* 101:17705–17710.
19. Sweet MJ, Leung BP, Kang D, Sogaard M, Schulz K, Trajkovic V, Campbell CC, Xu D, Liew FY (2001) *J Immunol* 166:6633–6639.
20. Chuang TH, Ulevitch RJ (2004) *Nat Immunol* 5:495–502.
21. Kobayashi K, Hernandez LD, Galan JE, Janeway CA, Jr, Medzhitov R, Flavell RA (2002) *Cell* 110:191–202.
22. Nakagawa R, Naka T, Tsutsui H, Fujimoto M, Kimura A, Abe T, Seki E, Sato S, Takeuchi O, Takeda K, *et al.* (2002) *Immunity* 17:677–687.
23. Wang YY, Li L, Han KJ, Zhai Z, Shu HB (2004) *FEBS Lett* 576:86–90.
24. Lin R, Yang L, Nakhaei P, Sun Q, Sharif-Askari E, Julkunen I, Hiscott J (2006) *J Biol Chem* 281:2095–2103.
25. Zhao H, Li CC, Pardo J, Chu PC, Liao CX, Huang J, Dong JG, Zhou X, Huang Q, Huang B, *et al.* (2005) *J Immunol* 174:5288–5297.
26. Zhao C, Denison C, Huibregtse JM, Gygi S, Krug RM (2005) *Proc Natl Acad Sci USA* 102:10200–10205.
27. Kumar S, Kao WH, Howley PM (1997) *J Biol Chem* 272:13548–13554.
28. Chin LS, Vavalle JP, Li L (2002) *J Biol Chem* 277:35071–35079.
29. Tanaka K, Suzuki T, Chiba T, Shimura H, Hattori N, Mizuno Y (2001) *J Mol Med* 79:482–494.
30. Niwa J, Ishigaki S, Doyu M, Suzuki T, Tanaka K, Sobue G (2001) *Biochem Biophys Res Commun* 281:706–713.
31. Urano T, Saito T, Tsukui T, Fujita M, Hosoi T, Muramatsu M, Ouchi Y, Inoue S (2002) *Nature* 417:871–875.
32. Moynihan TP, Ardley HC, Nuber U, Rose SA, Jones PF, Markham AF, Scheffner M, Robinson PA (1999) *J Biol Chem* 274:30963–30968.
33. Zhang Y, Gao J, Chung KK, Huang H, Dawson VL, Dawson TM (2000) *Proc Natl Acad Sci USA* 97:13354–13359.
34. Kotaja N, Karvonen U, Janne OA, Palvimo JJ (2002) *Mol Cell Biol* 22:5222–5234.
35. Kato H, Sato S, Yoneyama M, Yamamoto M, Uematsu S, Matsui K, Tsujimura T, Takeda K, Fujita T, Takeuchi O, Akira S (2005) *Immunity* 23:19–28.
36. Dastur A, Beaudenon S, Kelley M, Krug RM, Huibregtse JM (2006) *J Biol Chem* 281:4334–4338.

Journal of General Virology (2007), **88**, 3323–3333 DOI 10.1099/vir.0.83056-0

Hepatitis C virus non-structural proteins responsible for suppression of the RIG-I/Cardif-induced interferon response

Megumi Tasaka,[1]† Naoya Sakamoto,[1,2]† Yoshie Itakura,[1,3] Mina Nakagawa,[1,2] Yasuhiro Itsui,[1] Yuko Sekine-Osajima,[1] Yuki Nishimura-Sakurai,[1] Cheng-Hsin Chen,[1] Mitsutoshi Yoneyama,[4] Takashi Fujita,[4] Takaji Wakita,[5] Shinya Maekawa,[3] Nobuyuki Enomoto[3] and Mamoru Watanabe[1]

Correspondence
Naoya Sakamoto
nsakamoto.gast@tmd.ac.jp

[1]Department of Gastroenterology and Hepatology, Tokyo Medical and Dental University, Tokyo, Japan

[2]Department for Hepatitis Control, Tokyo Medical and Dental University, Tokyo, Japan

[3]First Department of Internal Medicine, University of Yamanashi, Yamanashi, Japan

[4]Laboratory of Molecular Genetics, Department of Genetics and Molecular Biology, Institute for Virus Research, Kyoto University, Kyoto, Japan

[5]Department of Virology II, National Institute of Infectious Diseases, Tokyo, Japan

Viral infections activate cellular expression of type I interferons (IFNs). These responses are partly triggered by RIG-I and mediated by Cardif, TBK1, IKKε and IRF-3. This study analysed the mechanisms of dsRNA-induced IFN responses in various cell lines that supported subgenomic hepatitis C virus (HCV) replication. Transfection of dsRNA into Huh7, HeLa and HEK293 cells induced an IFN expression response as shown by IRF-3 dimerization, whilst these responses were abolished in corresponding cell lines that expressed HCV replicons. Similarly, RIG-I-dependent activation of the IFN-stimulated response element (ISRE) was significantly suppressed by cells expressing the HCV replicon and restored in replicon-eliminated cells. Overexpression analyses of individual HCV non-structural proteins revealed that NS4B, as well as NS34A, significantly inhibited RIG-I-triggered ISRE activation. Taken together, HCV replication and protein expression substantially blocked the dsRNA-triggered, RIG-I-mediated IFN expression response and this blockade was partly mediated by HCV NS4B, as well as NS34A. These mechanisms may contribute to the clinical persistence of HCV infection and could constitute a novel antiviral therapeutic target.

Received 4 April 2007
Accepted 27 July 2007

INTRODUCTION

Type I interferon (IFN) plays a central role in eliminating virus, not only following clinical therapeutic application but also as a cellular immune response (Samuel, 2001; Taniguchi & Takaoka, 2002). Hepatitis C virus (HCV) infection is characterized by persistence and replication of the virus in the liver, despite an intact host immune system (Alter, 1997). Indeed, even after administration of the currently most potent IFN reagents, as many as half of the patients are refractory to the treatment and fail to eradicate the virus (Fried *et al.*, 2002). These features have led to speculation that HCV escapes from or attenuates the host antiviral response (Katze *et al.*, 2002).

Cellular antiviral responses are primarily mediated by IFN and IFN-stimulated genes (ISGs), including 2,5-oligoadenylate synthetase, dsRNA-dependent protein kinase R (PKR) and MxA proteins, as well as by as yet uncharacterized genes (Itsui *et al.*, 2006; Stark *et al.*, 1998). A study of experimental chimpanzee HCV infection has shown that various cytokines and chemokines are induced in the liver during the course of acute HCV infection and its clearance, and that a considerable proportion of the genes is induced by type I IFN (Bigger *et al.*, 2001).

Control of expression of ISGs is mediated by binding of type I IFNs to their receptors. Following receptor binding, STAT1 and STAT2 are phosphorylated to form ISGF-3, which translocates to the nucleus and binds the IFN-stimulated response element (ISRE), located in the promoter/enhancer region of ISGs, and activates transcription of ISGs (Samuel,

†These authors contributed equally to this work.

2001; Taniguchi *et al.*, 2001; Taniguchi & Takaoka, 2002). ISRE-dependent gene expression is also mediated by binding of the ISRE by molecules such as IRF-1, IRF-3 and IRF-7 (Kanazawa *et al.*, 2004). IRF-3 is a transducer of virus-mediated signalling and plays a critical role in the induction of cellular antiviral responses (Lin *et al.*, 1998; Sato *et al.*, 2000; Taniguchi *et al.*, 2001; Yoneyama *et al.*, 1998). Transcriptional activation and suppression of IRF-3 are inversely correlated with the level of HCV replication *in vitro* (Yamashiro *et al.*, 2006). Following virus infection, IRF-3 is phosphorylated by two cytoplasmic kinases, TBK1 and IKKε (Fitzgerald *et al.*, 2003; Sharma *et al.*, 2003). The phosphorylated IRF-3 forms a homodimer, translocates to the nucleus and predominantly activates expression of the IFN-β gene and certain ISGs (Doyle *et al.*, 2002; Nakaya *et al.*, 2001; Taniguchi & Takaoka, 2002).

RIG-I is a recently identified cytoplasmic DExD/H box RNA helicase that participates in recognition of virus-related dsRNA as a pathogen-related molecular pattern (Yoneyama *et al.*, 2005). RIG-I contains two caspase-recruitment domains (CARDs) in the N terminus and a DExD/H box RNA helicase in the C terminus. MDA5 has been identified as another CARD-containing DExD/H box RNA helicase (Andrejeva *et al.*, 2004). More recently, an adaptor molecule of RIG-I and MDA5, Cardif (also known as IPS-I, MAVS and VISA), has been identified by four independent groups (Kawai *et al.*, 2005; Meylan *et al.*, 2005; Seth *et al.*, 2005; Xu *et al.*, 2005). On association with dsRNA, RIG-I or MDA5 causes conformational changes and homo-oligomerization, and binds the CARD of Cardif (Saito *et al.*, 2007). Cardif subsequently recruits the kinases TBK1 and IKKε, which catalyse phosphorylation and activation of IRF-3 (Yoneyama *et al.*, 1998).

The IRF-3-mediated IFN-β induction pathway could be a target for viruses to counteract antiviral responses and promote their replication in host cells. Ebola virus, bovine viral diarrhea virus (BVDV) and influenza A virus interfere with the activation of IRF-3 through interactions of their virus-encoded proteins (Basler *et al.*, 2003; Schweizer & Peterhans, 2001; Talon *et al.*, 2000). There are several reports that HCV proteins interact with IFN-mediated antiviral systems. The NS5A and E2 proteins have been reported to interfere with the action of IFN by inhibiting the activity of PKR (He & Katze, 2002). It was reported recently that the HCV NS34A protease blocks virus-induced activation of IRF-3, possibly by proteolytic cleavage of Cardif (Foy *et al.*, 2003; Meylan *et al.*, 2005).

The HCV subgenomic replicon is an *in vitro* model that simulates autonomous cellular replication of HCV genomic RNA (Lohmann *et al.*, 1999). Expression of the HCV replicon can be abolished by treatment with small amounts of type I and type II IFNs (Blight *et al.*, 2000; Frese *et al.*, 2002; Guo *et al.*, 2001), suggesting intact IFN receptor-mediated cellular responses. In contrast, viral expression persists in the absence of the exogenous IFN. Baseline expression levels of ISG were substantially decreased in cells expressing the HCV replicon compared with parental Huh7 cells (Kanazawa *et al.*, 2004). These findings led us to speculate that intracellular virus-induced antiviral responses are attenuated or caused to malfunction by the expression of viral proteins.

In this study, we investigated cell lines that support subgenomic HCV replication and HCV cell culture for the dsRNA-induced cellular IFN expression pathway. Here, we report that RIG-I- and Cardif-mediated IFN gene activation is uniformly attenuated in several replicon-expressing cell lines of different lineages and, more importantly, that the HCV NS4B protein is involved in the suppression of antiviral IFN responses.

METHODS

Plasmids. Plasmids pEF-flagRIG-I and ΔRIG-I expressed full-length and C-terminally truncated RIG-I protein, respectively (Yoneyama *et al.*, 2004). The plasmid pER-flagRIG-IKA (RIG-IKA) has a point mutation in the putative ATP-binding site of the RIG-I helicase domain and was used as a negative control for ΔRIG-I and RIG-I full transfection assays. Expression plasmids for full-length Cardif (Cardif), Cardif CARD (CARD) and CARD-truncated Cardif (ΔCARD) were provided by Dr J. Tschopp (University of Lausanne, Switzerland) (Meylan *et al.*, 2005). Expression plasmids for toll-like receptor 3 (TLR3) and TIR domain-containing adaptor inducing IFN-β (TRIF), the transmembrane receptor of dsRNA and the adaptor molecule of TLR3, respectively, were provided by Dr S. Akira (Osaka University, Japan). Plasmids expressing HCV NS345, NS3, NS34A, NS4A, NS4B, NS5A and NS5B were amplified from HCV pCV-J4-L4S (Yanagi *et al.*, 1997) by PCR and subcloned. The DNA fragments were inserted into the vector pcDNA4/TO/*myc*-His (Invitrogen). Nucleotide sequences were confirmed by sequencing. Plasmids TOPO-NS34A (HCV N), TOPO-NS4B (HCV N) and pcDNA-NS4B (HCV JFH1) expressed Myc-tagged NS34A and NS4B proteins derived from the HCV N (Beard *et al.*, 1999) and HCV JFH1 (Wakita *et al.*, 2005) strains, as indicated. Plasmid pISRE-TA-Luc (Invitrogen) contained five copies of consensus ISRE motifs upstream of the firefly luciferase gene. Plasmid pIFNβ-Fluc was constructed by cloning the human IFN-β promoter region, spanning nt −110 to −36, upstream of the firefly luciferase gene of pGL3 Basic (Promega). Plasmid pcDNA3.1 (Invitrogen) was used as an empty vector for mock transfection. pRL-CMV (Promega), which expressed the *Renilla* luciferase protein, was used for correction of transfection efficiency.

Cell culture. HCV strain JFH1-infected Huh7.5.1, Huh7, Huh7.5.1 (kindly provided by Dr F. Chisari, The Scripps Institute, CA, USA; Zhong *et al.*, 2005), HeLa and HEK293 cells were maintained in Dulbecco's modified minimal essential medium (Sigma) supplemented with 2 mM L-glutamine and 10 % fetal calf serum at 37 °C with 5 % CO_2. Cells expressing the HCV replicon were cultured in medium containing 100 μg G418 (Wako) ml^{-1}.

HCV replicon constructs and transfected cell lines. An HCV subgenomic replicon plasmid, pHCVIbneo-delS (designated pRep-N), was derived from an HCV clone of strain N, genotype 1b, and pSGR-JFH1 was derived from HCV JFH1, genotype 2a (Guo *et al.*, 2001; Wakita *et al.*, 2005). These replicons were reconstructed by substituting the neomycin phosphotransferase gene with a fusion gene comprising *Renilla* luciferase and neomycin phosphotransferase to construct pRep-Reo-1b and pRep-Reo-2a, respectively (Tanabe *et al.*, 2004; Yokota *et al.*, 2003). RNA was synthesized from the replicons using T7 polymerase (Promega) and transfected into Huh7,

HeLa and HEK293 cells. After culture in the presence of G418, cell lines stably expressing the replicon were established (Huh7/1bReo, Huh7/2aReo, HeLa/2aReo and 293/2aReo). We have previously reported that firefly luciferase activities of Feo-replicon-expressing cells correlate well with HCV NS3, NS4A and NS5A protein expression levels and with the levels of replicon RNA (Yokota *et al.*, 2003).

Transient transfection. Transient DNA transfection was performed using Lipofectamine 2000 (Invitrogen) according to the manufacturer's protocol. ISRE reporter assays were carried out as previously described (Nakagawa et al., 2004). To analyse IFN expression in HCV JFH1 cell cultures, a total of 1×10^5 Huh7.5.1, JFH-1 infected Huh7.5.1 and IFN-treated Huh7.5.1 cells were seeded into 24-well plates the day before transfection. Plasmids pISRE-TA-Luc and ΔRIG-I (200 ng each) were transfected using 1 μl Lipofectamine 2000. RIG-IKA was used as a control. Luciferase assays were performed on day 3 post-transfection.

For further study, 400 ng of each non-structural protein was added to 1×10^4 Huh7 or HEK293 cells that had been seeded into 96-well plates the day before transfection. pISRE-TA-Luc and ΔRIG-I (40 ng each) were transfected using 0.5 μl Lipofectamine 2000. RIG-IKA was used as a control.

Western blotting. Preparation of the cytoplasmic and nuclear fractions of cell lysates was carried out as described previously (Tanabe *et al.*, 2004). Protein (20 μg) was separated using NuPAGE 4–12 % Bis/Tris gels (Invitrogen) and blotted onto an Immobilon PVDF membrane (Roche). The membrane was immunoblotted with anti-IRF-3 (Santa Cruz) and detected by chemiluminescence (BM Chemiluminescence Blotting Substrate; Roche).

RT-PCR. Interleukin (IL)-8 mRNA was detected by RT-PCR as described previously (Itsui *et al.*, 2006). The primers used were IL8-S (5′-GCACAAACTTTCAGAGACAGCAGAGCACAC-3′) and IL8-AS (5′-CAGAGCTGCAGAAATCAGGAAGGCTGCCAA-3′).

Indirect immunofluorescence assay. Cells seeded onto tissue culture chamber slides were fixed with cold acetone. The cells were incubated with anti-protein disulphide isomerase (PDI) or anti-Myc antibodies and subsequently with Alexa 488- or Alexa 568-labelled secondary antibodies. Cells were mounted with VECTA SHIELD Mounting Medium and DAPI (Vector Laboratories) and visualized by fluorescence microscopy (BZ-8000; Keyence).

Luciferase reporter assays. Luciferase activity was measured using a 1420 Multilabel Counter (ARVO MX; PerkinElmer) using a Bright-Glo Luciferase Assay System (Promega) or a Dual Luciferase Assay System (Promega). Assays were carried out in triplicate and the results expressed as means ± SD.

MTS assay. To evaluate cell viabilities, dimethylthiazol carboxymethoxyphenyl sulfophenyl tetrazolium (MTS) assays were performed using a CellTiter 96 AQueous One Solution Cell Proliferation Assay kit (Promega) according to manufacturer's instructions.

Statistical analyses. Statistical analyses were performed using an unpaired, two-tailed Student's *t*-test. *P* values of less than 0.05 were considered to be statistically significant.

RESULTS

IRF-3 dimer formation is attenuated in cells expressing the HCV replicon

In the HCV replicon-expressing cell lines Huh7/Rep-Reo-2a, Hela/Rep-Reo-2a and 293/Rep-Reo-2a, replicon expression levels corresponded well to internal *Renilla* luciferase activities. Expression of the HCV replicon was suppressed by IFN in a dose-dependent manner (data not shown).

Activation of RIG-I or MDA5 induces phosphorylation and homodimerization of IRF-3. Following transfection of poly(I : C) into Huh7, HeLa or HEK293 cells, IRF-3 dimers were detected (Fig. 1). However, in cells supporting HCV replicons, IRF-3 dimer formation was almost completely abolished. These findings showed that expression of HCV proteins blocked activation of dsRNA-mediated IFN expression and that these effects were consistently found in several cell lines of different origin.

The HCV replicon suppresses RIG-I/Cardif-induced IFN responses

ISRE reporter activities did not increase in naïve Huh7, HeLa or HEK293 cells following transfection of poly(I : C), whilst overexpression of full-length RIG-I increased poly(I : C)-mediated ISRE reporter activity in Huh7 and HEK293 cells (data not shown). In RIG-I-overexpressing Huh7 cells, transduction with an HCV replicon abolished the poly(I : C)-induced ISRE activation, and elimination of the replicon by IFN treatment restored these ISRE responses (Fig. 2a). Consistent results were obtained by overexpression of ΔRIG-I, a constitutively active form. Transfection of ΔRIG-I in Huh7 and HEK293 cells induced ISRE activation, whilst these responses were abolished or significantly suppressed in cell lines expressing HCV replicons and were recovered by eliminating the replicon by IFN treatment (data not shown). Similarly, ISRE activation by overexpression of Cardif, an adaptor molecule of RIG-I, was almost completely blocked in replicon-expressing cells and was recovered by eliminating the replicon from the cells (data not shown). The RIG-I-mediated IFN response was

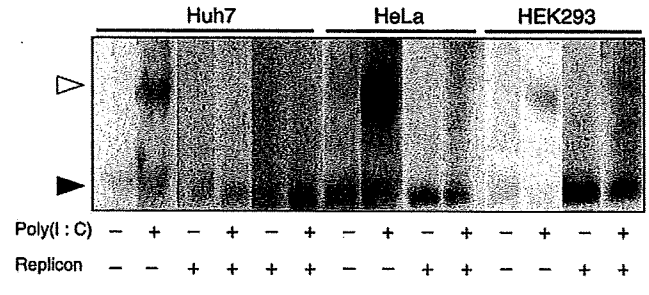

Fig. 1. Double-stranded RNA-induced IRF-3 dimer formation in cell lines that support HCV subgenomic replication. Poly(I : C) was transfected into naïve Huh7, HeLa and HEK293 cells, and into corresponding cell lines expressing the HCV replicon. Six hours after transfection, cell lysates were prepared, separated in polyacrylamide gels and blotted onto PVDF membrane. The membrane was immunoblotted with anti-IRF-3 and visualized by chemiluminescence (see Methods). The positions of the IRF-3 dimer (open arrowhead) and monomer (closed arrowhead) are indicated.

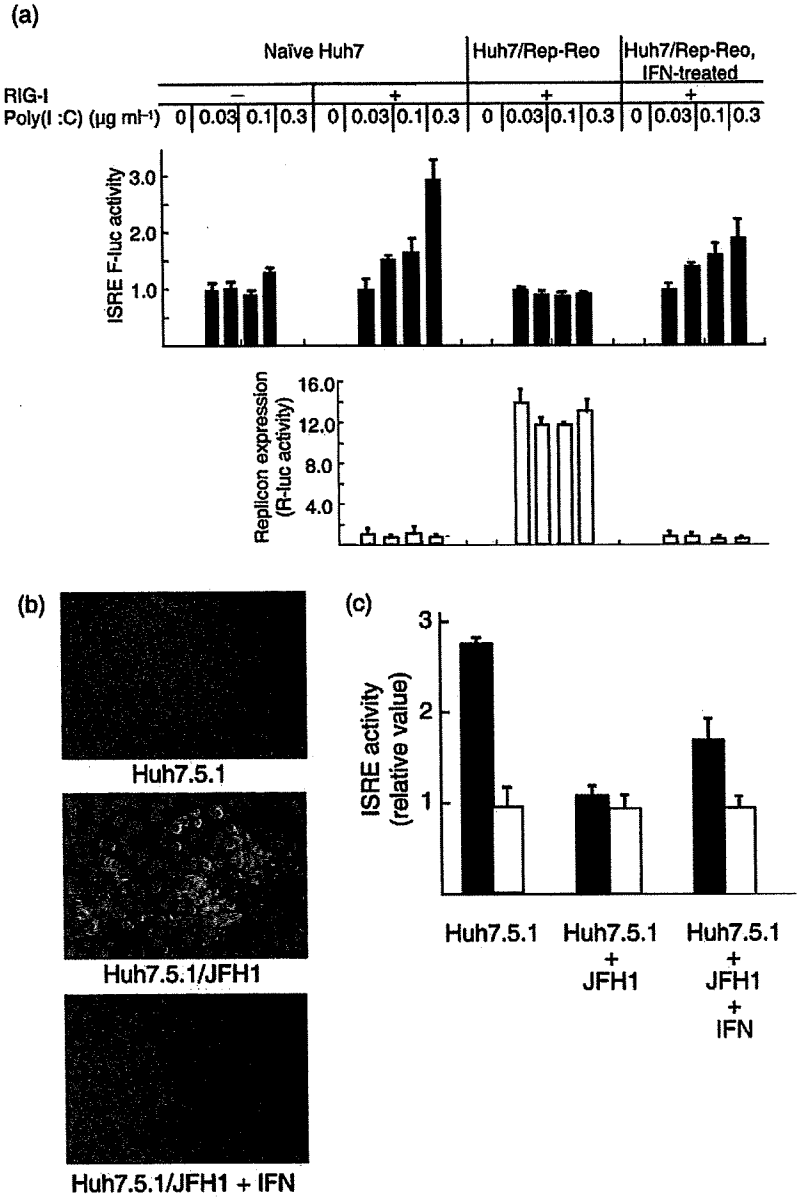

Fig. 2. Suppression of dsRNA-induced, RIG-I-mediated ISRE activation by HCV replication. (a) The HCV replicon suppresses transcriptional activation after poly(I : C) stimulation. The RIG-I expression plasmid and pISRE-TA-Luc were transiently transfected into the cell lines indicated. The following day, the amounts of poly(I : C) indicated were transfected into the corresponding cell lines and dual luciferase assays were carried out 8 h after transfection. Filled bars indicate ISRE-regulated firefly luciferase (F-luc) activities and open bars indicate *Renilla* luciferase (R-luc) activities representing replicon expression levels. In both graphs, scales for the *y*-axis are shown as relative values. Assays were carried out in triplicate and results are shown as means ± SD. (b) Immunofluorescence microscopy results. Huh7.5.1 cells infected with HCV JFH1 (Huh7.5.1/JFH1) and JFH1-infected cells from which the virus had been eliminated by IFN treatment (Huh7.5.1/JFH1 + IFN) were incubated with anti-core primary antibodies followed by Alexa Fluor-conjugated secondary antibody (green). Nuclei were stained with DAPI (blue). (c) ISRE activation by ΔRIG-I overexpression. The plasmid pISRE-TA-Luc was co-transfected with ΔRIG-I (filled bars) or RIG-IKA (empty bars) into naïve Huh7.5.1, Huh7.5.1/JFH1 or Huh7.5.1/JFH1 + IFN cells. Luciferase assays were carried out 8 h after transfection. The *y*-axis indicates ISRE-regulated luciferase activity shown as relative values. Assays were carried out in triplicate and results are shown as means ± SD.

also suppressed in HCV JFH1 virus cell culture. In JFH1-infected Huh7.5.1 cells, ΔRIG-I-induced ISRE reporter activation was significantly suppressed, but was recovered in IFN-treated, virus-eliminated cells (Fig. 2b and c). These results demonstrated that RIG-I- and Cardif-mediated antiviral responses were substantially suppressed by both subgenomic and genomic viral replication in both hepatocyte- and non-hepatocyte-derived host cells.

NS34A and NS4B are responsible for suppressing RIG-I-mediated IFN responses

We next sought to define which HCV proteins were responsible for inhibition of the RIG-I- and IRF-3-mediated IFN induction pathway. We constructed expression plasmids that expressed the non-structural proteins NS345, NS3, NS34A, NS4A, NS4B, NS5A and NS5B (Fig. 3a). We transfected each expression plasmid with simultaneous activation of the RIG-I pathway by overexpression of ΔRIG-I, Cardif, TBK1 and IKKε (Fig. 3b–e). Expression of full-length non-structural (NS345) and NS34A proteins inhibited ISRE activation mediated by expression of RIG-I and Cardif but not that mediated by TBK1 and IKKε. Interestingly, it was found that NS4B also inhibited ISRE activation mediated by expression of RIG-I and Cardif, but not by TBK1 and IKKε. Consistent with Fig. 3(b), overexpression of NS4B significantly suppressed ΔRIG-I-induced activation of the authentic IFN-β promoter (Fig. 3f).

Another group has studied IFN antagonism of flavivirus non-structural proteins and has reported that HCV NS4B did not affect IFN responses (Muñoz-Jordán *et al.*, 2005).